# GEOMORPHOLOGIC INVESTIGATIONS ON KARST TERRAIN: A GIS-ASSISTED CASE STUDY ON THE ISLAND OF BARBADOS

by

Hsin-Hui Huang
Department of Bioresource Engineering
Macdonald Campus, McGill University,
Montréal, Québec

A thesis submitted to McGill University in partial fulfilment of the requirements of the degree of Master of Science

*Your file Votre référence*
*ISBN: 978-0-494-32723-4*
*Our file Notre référence*
*ISBN: 978-0-494-32723-4*

# ABSTRACT

Maintaining a safe water supply is particularly crucial for karst islands such as Barbados. In order to take proper measures to prevent and reduce saltwater intrusion and to safely extract the right fraction of recharge, karst characteristics must first be fully understood. Geomorphologic investigations of karst surface features of the Porters & Trents groundwater catchments (Barbados) employed GIS technologies to explore the development and distribution of sinkhole features. Contour-based digital elevation models, surface geology, lithology, and remote sensing images were incorporated in this investigation. Seventy-six sinkholes were investigated and occupied approximately 1% (0.16 $km^2$) of the total area (16.41 $km^2$) under study. It was found that age of karstification is not related to age of a terrace. The middle terrace was the one found to be most karstified. Yet, degree of karstification within a terrace is age related. Also, cluster density increases with age of coral within the middle terrace. Density of sinkholes within a cluster also increases with age of coral within the middle terrace.

Finally, this study shows that sinkhole long axis, cluster elongation direction, sinkhole alignment and karst lineament all have a tendency to a northeast alignment. This supports the idea that underlying coral rock fracture and conduits have a northeast orientation.

## RÉSUMÉ

Le maintien d'un approvisionnement en eau potable est particulièrement crucial pour des îles de karst telles que les Barbades. Afin de prendre des mesures appropriées pour empêcher et réduire l'intrusion d'eau de mer et d'extraire sans risque une fraction adéquate de la recharge, des caractéristiques de karst doivent d'abord être entièrement comprises. Une étude géomorphologique des motifs karst de la surface des zones de captage d'eaux souterraines de Porters & Trents aux Barbades, employa des techniques SIG pour étudier le développement et la distribution de dolines. Un modèle altimétrique numérique fondée sur les contours, la géologie de surface, la lithologie, et des images télédétectées servirent dans cette étude. Soixante-dix-sept dolines, occupant environ 0.16 $km^2$ ($\approx$ 1.0%) d'une région totalisant 16.41 $km^2$ furent étudiées. L'ancienneté de karstification ne fut pas reliée à celle des terrasses; la terrasse intermédiaire étant la plus karstifiée. Toutefois, le degree de karstification à même une terrasse est relié à son ancienneté. De plus, sur la terrasse intermédiaire la densité de dolines dans une grappe augmenta avec l'âge du corail sous-jacent. Finalement, cette étude montra que l'axe principal, l'orientation d'élongation de grappe, l'alignement de dolines, et le linéament du karst tendèrent tous vers un alignement nord-est, appuyant l'idée que les fractures et conduits dans le corail-roc sous-jacent ont la même orientation.

# ACKNOWLEDGEMENTS

I would like to express my sincere gratitude and appreciation to Dr. Robert Bonnell, who provided me this extraordinary opportunity and experience to develop this thesis project. His support and patience during my thesis development make it possible to complete my thesis successfully. Many thanks due to my thesis examiners Dr. S. Prasher and Dr. G. Mehuys who provided me very constructive suggestions to improve this thesis.

The data and technical support provided by the Walter Hitschfeld Geographic Information Centre are gratefully appreciated. I also would like to express my special appreciation to Ms. Anastassia Khouri of McGill University for her help and encouragement to this thesis project and her pleasant friendship.

Many thanks are due to those Bajans with whom I worked during my journey in Barbados. The partial funding for this research received from the Department of Computer Science, Mathematics & Physics of the University of the West Indies (UWI) and the research guidance from Dr. Leo Moseley (UWI) are gratefully acknowledged. I would like to thank the staff of Barbados Water Authority, especially Mr. Barry L. Mayers for his field support under many rough conditions, his assistance during data collection and his friendship. I am grateful for both equipment and data support from Costal Zone Management Unit and Lands and Surveys Department of Barbados throughout my field work.

Finally, I would like to express my thanks to my husband Emmanuel. His countless understanding, support and encouragement throughout my study as well as his love and caring to me and our son make this thesis possible.

TABLE OF CONTENTS

## LIST OF TABLES

## LIST OF FIGURES

## LIST OF SYMBOLS AND ACRONYMS

| | |
|---|---|
| $\overline{A}$ | Mean sinkhole area ($m^2$) |
| $A_k$ | Area of studied karst lands ($km^2$) |
| $A_{si}$ | Area of an individual sinkhole ($m^2$) |
| $CaCO_3$ | Calcium Carbonate |
| $CaMg\ (CO_3)_2$ | Calcium Magnesium Carbonate |
| $d_c$ | Thickness of coral rock beneath an individual sinkhole (m) |
| $d_i$ | Elevation difference between values from interpolated DEM and true point (m) |
| $D_s$ | Sinkhole density ($km^{-2}$) |
| $L$ | Length of the long axis of a sinkhole (m) |
| $L_1$ & $L_2$ | Longest and shortest parts respectively of the sinkhole long axis on either side of the lowest point (m) |
| $\overline{L_a}$ | Mean actual distance between neighbouring sinkholes (m) |
| $\overline{L_e}$ | Mean expected distance between neighbouring sinkholes (m) |
| $\overline{L_{ec}}$ | Mean modified expected distance between neighbouring sinkholes (m) |
| $L_{sg}$ | Distance between sinkholes and nearby gullies (m) |
| ME | Mean error (m) |
| $n$ | Number of test points |
| $NH^{4+}$ | Ammonium Ion |
| $NO_3^-$ | Nitrate |
| $N_s$ | Numbers of the sinkholes in the karstic lands. |
| $P$ | Perimeter of a karst area |
| $P_s$ | Product of symmetry |
| $R_L$ | Length ratio |
| $R_p$ | Pitting index |
| $\overline{R}$ | Nearest neighbour index |

| | |
|---|---|
| $\overline{R_c}$ | Modified nearest neighbour index |
| $R_s$ | Sinkhole area ratio |
| $R_{\mathrm{LW}}$ | Aspect ratio |
| RMSE | Root mean square error (m) |
| $R_{\mathrm{W}}$ | Width ratio |
| TDS | Total dissolved solids |
| $W_1$ & $W_2$ | Longest and shortest parts respectively of the sinkhole width axis on either side of the lowest point, measured at right angles to the length axis (m) |
| $W_{\mathrm{max}}$ | The longest distance across, perpendicular to long axis of a sinkhole (m) |
| $Z_{\mathrm{int}}$ | Interpolated DEM elevation of a test point (m) |
| $Z_{\mathrm{true}}$ | True elevation of a test point (m) |
| $\delta_{18}O$ | The ratio of stable oxygen isotopes |

## SCOPE OF THE WORK

This thesis describes the development, application, and geographic information system-assisted (GIS) analysis of karst geomorphology in the Porters and Trents groundwater catchments on the island of Barbados. The study was conducted in conjunction with the Barbados Water Authority (BWA) and the University of the West Indies (UWI). The goal of this work was to develop a groundwater management project on the west coast of the island. Initially, the conceptual groundwater model implemented was restricted to the coast of these two catchments due to limited hydrogeologic data. In order to provide a hydrogeologic framework upon which regional groundwater flow in this aquifer could be better understood, this study focused on establishing a GIS-based karst database and obtaining a quantitative description of the karst formation within the catchments of interest.

With only three months available for data collection in the area studied, the major focuses of this work were topographic formation and geomorphologic development of karst surface features, especially sinkholes and gullies. Other data such as lithologic information, hydrologic boundaries, and anthropogenic aspects were also included. This work represented an initial attempt to integrate hydrogeologic information on a karst terrain using a GIS, with the potential for future incorporation of greater complexity and to address additional groundwater management problems.

# CHAPTER 1 INTRODUCTION

## 1. 1 Research motivations and objectives

The term 'karst' is generally used as a synonym for barren rocky terrains. These types of terrains are generally considered not suitable for large scale development such as hydro projects (i.e., dams, reservoirs or water supply) due to the complex geological features and unique hydrological characteristics of carbonate rocks. However, rising world-wide demands on drinking water, land, and energy keep drawing interest to the exploration of karst resources, particularly for water-supply.

According to the Millenium Development Goals (MDGs), countries, including those in the Caribbean, commit themselves to halve the portion of their population without access to a safe water supply by the year 2015 (Ringskog, 2004). This situation is particularly crucial for karst islands such as Barbados because of the absence of surface water, drought during the dry season and pollution from various sources (White, 1988). The Inter-American Agency for Cooperation and Development (IACD) of the Organization of American States (OAS) funded three Caribbean islands to seek management strategies and methodologies so that coastal karst aquifers can be sustained. Since 2002 three islands: Barbados, Antigua, and Jamaica have made efforts to minimize saltwater intrusion. In order to take proper measures to prevent and reduce saltwater intrusion and to safely extract the right fraction of recharge, karst characteristics must first be fully understood.

On the island of Barbados, two catchments located along the west coast of the island, Porters and Trents, were chosen by the staff of the Barbados Water Authority (BWA) to implement a sustainable groundwater management model study. As karst formation and evolution are a consequence of water dissolution of the carbonate media, studying karst hydrogeology is uniquely challenging. LaMoreaux *et al.* (1997) stated that, given the complex hydrogeologic nature of karst terrains, concepts related to the movement and occurrence of groundwater or methods used in the management and development of water sources cannot be based on a single uniform set of rules. Consequently, a full understanding of karst geomorphology is a prerequisite in solving hydrogeologic and geotechnical problems (Milanovic, 2004). In 1989, Waltham found that groundwater flow patterns and subterranean geology features can be estimated via geomorphologic analysis of surface features. Yet a full understanding of karst groundwater flow in karst terrains has not been attained.

This current study was undertaken in conjunction with BWA and the University of the West Indies (UWI) to perform a geomorphologic characterization of the two aforementioned catchments on the island of Barbados using a geographic information system (GIS). GIS is capable of manipulating large data sets and is becoming an important component of karst studies. The karst terrain of Barbados is somewhat unique. The aerial extent is quite limited (432 km$^2$) and surrounded by ocean. Furthermore, Barbados has a "coral cap", a coral limestone formation capping the landscape, covering 85 % of the island and up to 100 m thick, with porosity of 20-60 % (Jones, 2003). This coral cap is karstified, and various karst surface features such as sinkholes, gullies, springs and caves are evident.

Therefore, the overall goal of this research was to investigate the development and distribution of surface karst features using GIS tools; with the expectation that such analysis will be helpful to future groundwater flow studies. The specific objectives were to determine: (i) the controls on karst evolution, particularly in terms of sinkhole development, (ii) the characteristics of sinkhole geometry as well as the factors which promote sinkhole enlargement, (iii) the specific geologic features which promote sinkhole occurrence, and (iv) the limitations in spatial distribution of sinkholes in terms of pattern, spatial relationships with dry gullies, long-axis orientation of sinkholes, and sinkhole alignment.

## 1. 2 Knowledge regarding karst

### 1. 2. 1 Historical evolution of karst knowledge

The term karst has been used worldwide since the early part of the 19th century to describe terrain with distinctive hydrology and landforms produced on highly soluble rocks including limestone, dolomite, gypsum, halite, and conglomerates. The origin of the word "karst" can be traced back to a century ago in different derivatives of European and Middle Eastern languages, such as the use of 'karra' to refer to stone. The region- kras (between Yugoslavia and Italy) was the first karstland to receive intensive scientific investigations for its natural characteristics, and hence was viewed as a "classical karstic terrain". The word, afterward, evolved to karst with the Germans and typically was used to describe terrains or landforms underlain by limestone, dolomite or other soluble material.

Typical karstic topography consists of streams, caves, enclosed depressions, fluted rock outcrops and large springs (Ford and Williams, 1989). Areas underlain by gypsum, halite, or quartz sandstone can also form karstic terrains. Limestone consists mainly of $CaCO_3$ and dolomite of $CaMg\ (CO_3)_2$, formed by the deposition of organic matter (shells and corals). Tectonic processes often fracture sedimentary rocks. This process is often fairly rapid in carbonate rocks, and water entering these cracks gradually dissolves the surrounding rocks creating wider and deeper cracks ("*Karst Management Handbook for British Columbia*", 2003). The development of karst is largely determined by geologic processes, by climate factors and by types of carbonate rocks.

Karst aquifers are those that contain dissolution-generated conduits that permit the rapid transport of groundwater, often in turbulent flow. A conduit can be defined as pipe-like openings with apertures ranging form one centimeter to a few decameters (White, 1988). The conduit system often receives localized runoff via sinkholes. Also, the conduit system interconnects with the groundwater stored in fractures and in the granular permeability (matrix flow) of the bedrock. In the early 90s, the research on karst aquifers was mainly focused on the quantification of conceptual models as well as the equilibrium chemistry of limestone and dolomite dissolution. Modeling of groundwater flow in karstic aquifers has been less than entirely successful (White, 1988). Progress has been made in the use of water budgets, tracer studies, hydrograph analysis and chemograph analysis for the characterization of karst aquifers (White, 1988; Jones, 2003; Milanovic, 2004).

In the 20$^{th}$ century, karstlands received a great deal of attention from a diverse array of scientists in fields including hydrology, geology, geochemistry, geomorphology, etc. New methods have employed sequential satellite imagery, aerial photography, remote sensing, computers, and results from sophisticated chemical laboratories, isotope hydrology and model analysis. Karst processes have been explained in detail by Jennings (1975 & 1985), Williams (1969), Ford & Williams (1989) and Milanovic (2004).

### 1. 2. 2 Benefits and damages from karst

Karst areas cover about 25% of the world's land surface of the world (Ford and Williams, 1989). They are among the Earth's most diverse, scenic and resource-rich terrains. In general, water resources are the major interest in karst exploitations. Karst regions are inherently complex in their hydrogeologic characteristics and therefore the management of the water they bear is difficult. Water management is particularly essential on a small karst island such as Barbados, where there is little surface water, there have been several droughts during dry seasons, and there are numerous sources of pollution ("*GEO Barbados*", 2000). Other types of natural karst resources, such as various forms of mineral deposits, are found in caves. Exploration activities for oil and gas are especially important on karst. Apart from their rich natural resources, the karst subsurface environment offers many opportunities for scientific and educational research as well as recreational benefits ("*Karst Management Handbook for British Columbia*", 2003).

Karstlands are generally more environmentally sensitive than other rock terrains. The unique hydrogeologic characteristics make karst aquifers particularly vulnerable to pollution, often brought on by human activities around unprotected sinkholes. Sinkholes (referred to as 'doline' in European literature), the result of bedrock dissolution or the collapse of shallow cavern roofs (Williams, 1969), are relatively shallow, bowl-shaped depressions ranging from a few meters to a kilometer in diameter, and up to hundreds of meters in depth. The drain-ways from many sinkholes are interconnected with underlying conduit systems resulting in rapid and direct water infiltration into the conduit network. As a result, the attenuation of contaminants does not occur as effectively as in porous aquifers. This rapid transit time and limited natural cleansing and filtering mechanisms associated with subsurface stream systems can readily transport harmful materials, such as contaminants or sediments, from one area to another. These materials potentially have a serious impact on sensitive karst environments, especially water supplies. Unfortunately, unprotected sinkholes are, in many cases, used as farm lands or for waste disposal. Additionally, high urbanization on karst can result in a serious sinkhole flooding problem which occurs during a steep rising limb of a flood hydrograph. Because of the rapid response time of open conduit systems, flooding in caves and sinkholes has much the same characteristics. Rapid internal runoff through sinkholes and sinking streams fill the main conduit system much faster than the diffuse flow in smaller openings and fractures can receive. Closed depressions flooded by rising regional water levels often remain flooded for long periods of time.

Furthermore, over-extraction of groundwater from karst coastal aquifers can lead to a serious problem of saltwater intrusion. Depending on levels of natural recharge/discharge thresholds, saltwater intrusion can take place at the outlets or, more inland, at greater depths. Due to sea level rise, some karst springs which long ago occurred at the land surface are now submarine. In general, the greater the outflow of karst springs, the lower the salinity of the out-flowing water. Mixing of fresh and saline water takes place rapidly, rendering the out-flowing fresh water unfit for use (Milanovic, 2004).

## 1. 3 General description of Barbados

### 1. 3. 1 Geographic and climatic setting

Barbados is the most easterly island in the Caribbean Sea, centered at 13°10' N and 59°35' W (Figure 1-1). Its total area is about 432 km$^2$ with 92 km of coastline; the island extends approximately 34 km in length and is 23 km in width. The highest point of the island is about 340 m above mean sea level. The climate in Barbados is classified as being sub-humid to humid and oceanic tropical, with mean annual temperatures between 24°C and 28°C ("*GEO Barbados*", 2000). The weather can be divided into two seasons: the dry season from December to May and the wet season from June to November. On average, 78% of the total annual rainfall accumulates during the wet season. The annual mean rainfall is 1650 mm at high elevations and 1254 mm at lower elevations (Figure 1-2) (Jones *et al.*, 2000; Jones, 2003).

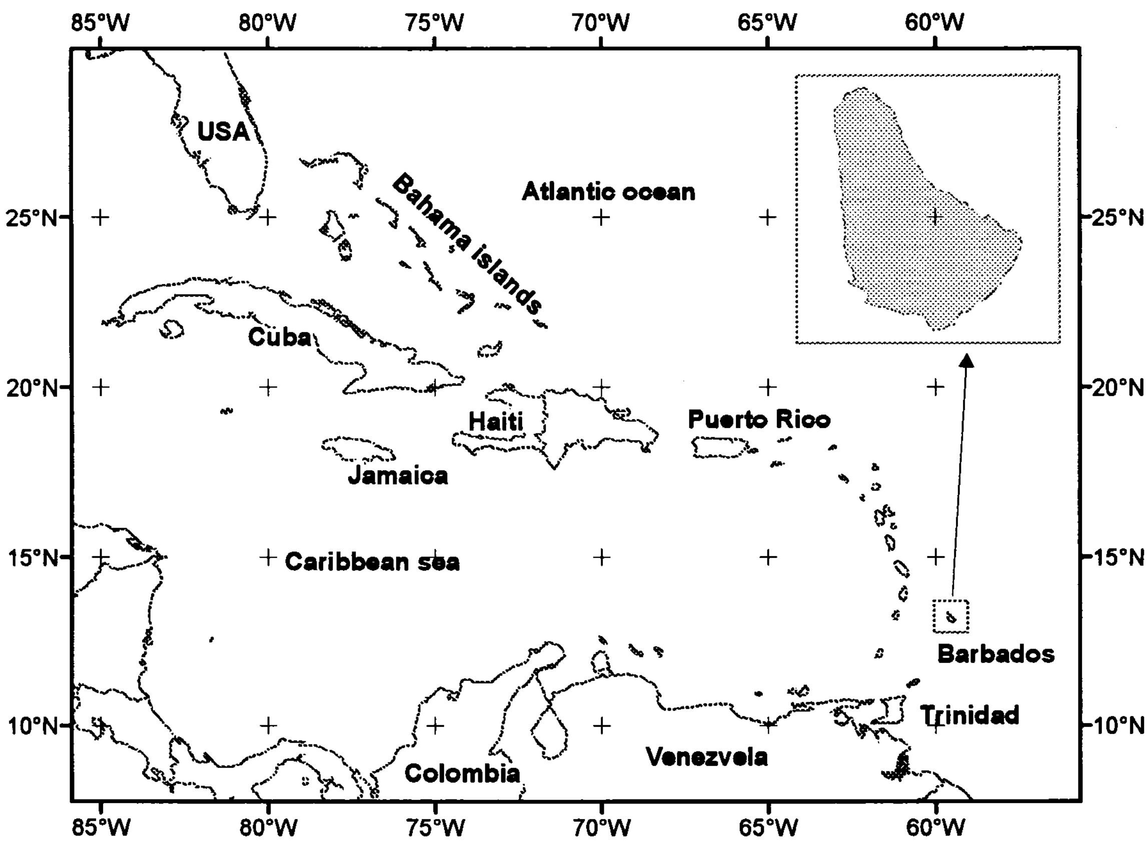


**Figure 1-1:** A map of the Caribbean Sea

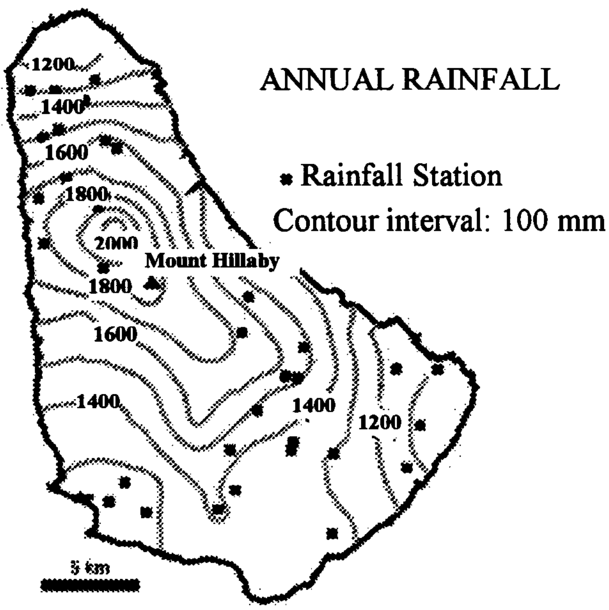


**Figure 1-2:** The distribution of annual rainfall (mm) on the island of Barbados in 1992 (obtained from Jones, 2003)

### 1. 3. 2 Hydrogeologic setting

Differing from its Lesser Antillian neighbours, Barbados presents distinct geological formation and topographical characteristics. Coralline limestone outcrops occur over 85% of the island, including an Upper reef terrace, a Middle reef terrace and a Lower reef terrace (Figure 1-3); locals refer to these areas as the 'Coral Cap'. The Scotland District (occupying 15% of the land surface) situated in the north-eastern portion of the island has been eroded to reveal the underlying sandstones and clay (Fermor, 1972). The Coral Cap descends toward the west and south in a series of terraces from the highest points of 340 m. The westerly movement of the North American plate against the easterly moving Caribbean plate has been raising the island at a uniform rate of 0.3 m per thousand years (Mesolella, 1967). Significant tectonic movements which occurred in the Pleistocene separated the coral-deposited formation into three levels of terraces, exposing the First and Second High Cliffs (Day, 1983), which are clearly visible. The thickness of the coral cap is up to 100 m (Jones *et al.*, 2000; Jones, 2003).

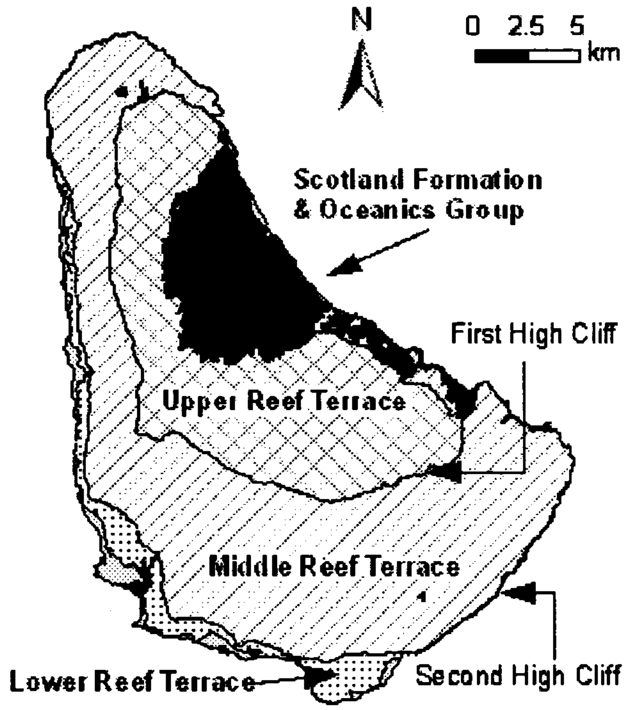


**Figure 1-3:** Surface geology of Barbados

Like other karstlands, the characteristics of hydrology on the island are mainly controlled by its geological formations. The Scotland District, consisting of fine grained clays and shale, has a lower infiltration rate and permeability than Coral Cap areas. Senn (1946) divided the Coral Cap into two hydrologic zones - stream-water and sheet-water zones (Figures 1-4 & 1-5), with respect to phreatic conditions. In the first case, water percolates through the coral until arrested by the Oceanics beneath (deep-water limestones of low permeability). This water flows seaward diffusely in fracture and matrix flow or more directly via conduit flow (Figure 1-4). The water table in this zone is approximately 30 m below the valley floors and closely tied to the top of the Oceanics (Fermor, 1972). The sheet water zone starts where the surface of the Oceanics is below sea level. The water table in this zone is closely paralleled to and just above sea level (Senn, 1946). At the inland part of the sheet-water zone, the water table is about 50 m below the valley floors and about 1 m above sea level. In wet seasons it may rise a further metre or two. The location of the interface between fresh water and saltwater is governed by the permeability of the coral rock, the amount of percolation, and the amount of extraction.

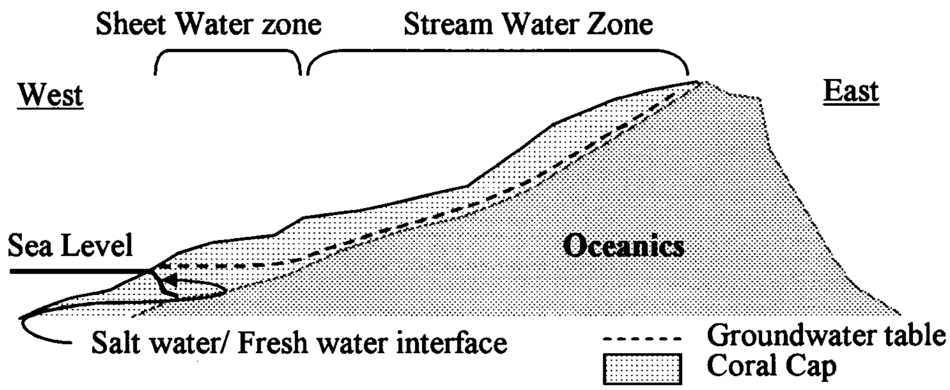


**Figure 1-4:** A typical hydrologic profile of the Coral Cap on the island of Barbados

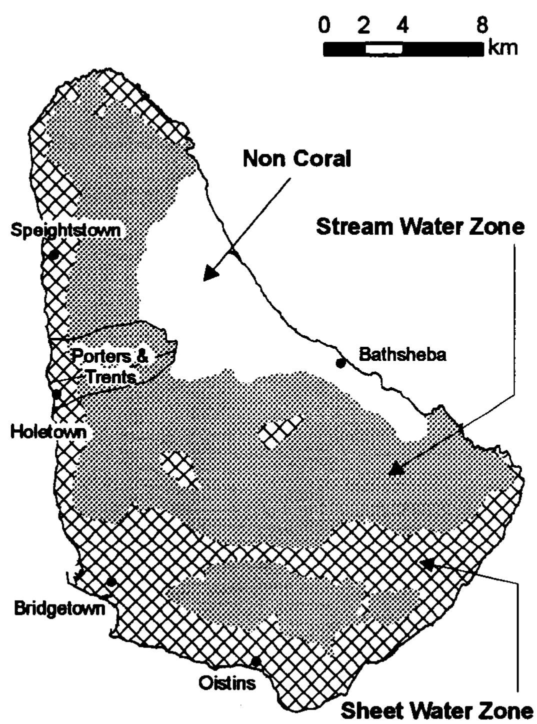


**Figure 1-5:** The distribution of the sheet water and stream water zones

In addition to hydrologic zones, the aquifer has been subdivided into twenty-two groundwater catchments ("*Water Resources and Hydrogeology*", 1978) based on the topography of the Coral Cap base (Figure 1-6). The topography of the top of the aquitard was assumed to govern the flow patterns in the aquifer. The ridges in the topography of the top of aquitard thus form the boundaries of the catchments (Jones *et al.*, 2000).

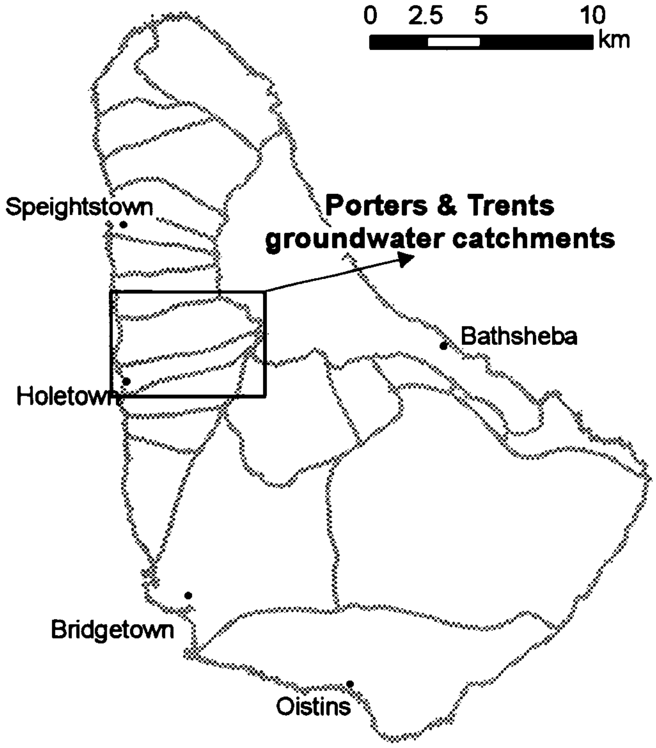


**Figure 1-6:** Twenty-two groundwater catchments of Barbados

## 1. 3. 3 Socio-economic context

Being one of the most densely populated countries in the world (623 people /km$^2$), Barbados has successfully controlled its population growth ("*GEO Barbados*", 2000). A family planning implementation along with its overall economic development have attained an annual population grow rate at 0.3 % during past twenty years.

Traditionally the economy of the island relies on its natural resources which have supported the agricultural industry for decades. However, given the decline of the sugar cane industry, tourism is gradually replacing the traditional economy. From 1970 to 1999, the ratio of stay-over tourists to local population increased from 0.7:1 to 2:1. Tourism, playing an important role in the social-economic development of Caribbean countries, accounts for about 40% of the regional Gross Domestic Product. Tourism largely depends on a sustainable and safe water supply. In 2000, Barbados was classified by the World Bank as an upper middle-income country with its gross national product (GNP) per capita of 8,620 US$/year (Moore *et al.*, 2003). Other economic components, such as small scale fisheries and recently exploited petroleum reserves, also contribute to Barbados' economy. Nevertheless, the dense population and economic activities have been exerting pressures on the quality of the environment.

As described by Moore *et al.* (2003), the environmental impacts are correlated to increased income, population density, and economic activities. The impacts on the state of water resources, groundwater contamination, energy consumption, waste generation and disposal, as well as marine environments are evident. Rationalisation and management strategies are needed to achieve sustainable development and to maintain the quality of life on the island.

### 1. 3. 4 Water scarcity and groundwater contamination

Barbados has been listed as one of the most "water scarce" countries in the world (Moore *et al.*, 2003). The amount of freshwater in Barbados is influenced by its tropical climate and hydrogeologic conditions. The fundamental source of potable water is contributed by wet-season rainfall (June to October). Based on 1947-1994 rainfall data, the annual renewable freshwater resource was estimated to be 187,700 $m^3$ $d^{-1}$ ("*GEO Barbados*", 2000). In 2000, approximately 169,600 $m^3$ $d^{-1}$ was extracted from wells or boreholes for public (132,500 $m^3$ $d^{-1}$) and private (37,100 $m^3$ $d^{-1}$) uses. Most of the wells, typically vertical shafts about 2-3 m in diameter, were hand-dug and constructed more than 100 years ago (Senn, 1946). In order to meet the increasing water demand, the brackish water desalination facility "Spring Garden Plant," having the greatest capacity in the Caribbean (30,000 $m^3$ $d^{-1}$), has begun to provide a water supply to 20% of the population since 2000 (Bernitz, 2000). Nevertheless, the demands from residential, commercial, touristic and industrial developments are estimated to reach 203,650 $m^3$ $d^{-1}$ (146,900 $m^3$ $d^{-1}$ for public; 56,750 $m^3$ $d^{-1}$ for private) by 2016 ("*GEO Barbados*", 2000).

Salinity tests of extracted groundwater conducted by Farrell *et al.* (2002) revealed that groundwater abstraction on the island has exceeded the sustainable yield. This could result in a worsening of seawater intrusion, which has been going on for several decades, into the aquifer systems of Barbados. As part of the strategic plans on sustaining groundwater resources, a pumping restriction will be imposed when a well's salinity exceeds 250 mg $L^{-1}$. In order to avoid regional water shortages, particularly during the dry season, there is an urgent need to characterize the karst aquifer (Farrell *et al.*, 2002). Furthermore, the maintenance of water distribution networks assumed to have leakage of up to 62 % of the pumped volume is another serious concern regarding the management of water resources (Klohn, 1998).

Apart from maintaining the water quantity, a zoning system based on the bacteriological attenuation rate of groundwater flow within limestone to pumping wells was implemented in 1963. This zoning system is used to protect groundwater quality from bacteriological contamination, but not from chemical pollution. The island is divided into five zones (Figure 1-7), zone 1 being the most restrictive to physical development. The determination of zoning boundaries and domestic control restrictions are described in Appendix A. According to *GEO Barbados* (2000), the quality of potable groundwater met international standards of biologically safe water for the parameters listed in Appendix B. It was concluded that the zoning system was effective in protecting the public from indicator diseases such as cholera, dysentery, giardiasis or hepatitis.

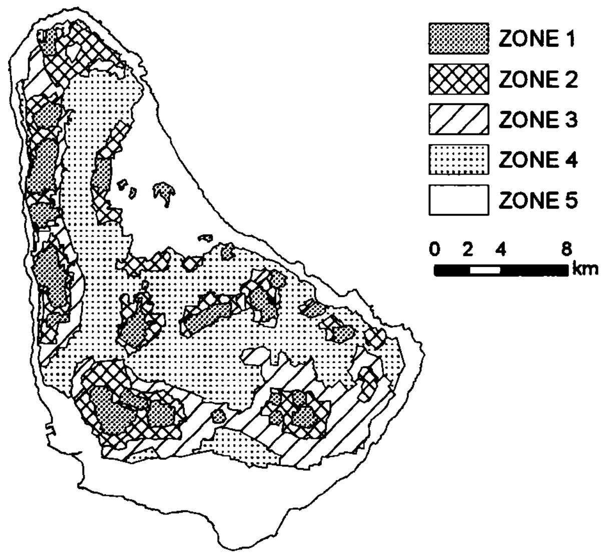


**Figure 1-7:** Five groundwater protection zones

Nevertheless, the consequence of a lack of regulations on chemical source control is an upward trend of chemical concentration in drinking water, in particular the level of nitrates and atrazine. Unregulated agricultural activity, petrochemical industry, industrial activity, hazardous wastes, urban development and waste disposal located in or around Zones 1 and 2 have increased rapidly. Intensive agriculture practices have been reported to be responsible for most of the increase in nitrate levels since 1977 ("*GEO Barbados*", 2000). Industries surveyed indicated that 34% of small scale operations handling chemicals, such as lead oxide, nickel sulphonate, photographic developer, fenithronthion, etc, are situated in Zones 1, 2 and 3. Yet, there is no waste generation reported.

Additionally, the leachate escaping from landfills (the used disposal method in Barbados) is posing a serious threat to water quality. One of the unlined official landfills (i.e., Mangrove I) and several unofficial operations located near pumping wells of Zone 1 are potential sites for contamination of groundwater.

## 1. 4 General description of the study area

The study area was made up of the Trents and Porters groundwater catchments (Figure 1-6) located along the west coast of the island. This site extends from the coastline to approximately 7 km inland, and is covered by recent and marine deposits of calcareous sand and coral fragments ranging from 0.5 m to 18 m in thickness. Beneath the sediment deposits is highly permeable coral rock ranging from 50 m to more than 100 m in thickness in regions distal from the coast. Numerous surface karstic features (i.e., sinkholes and dry gullies) transport significant volumes of water into subtending aquifers after substantial rainfall. Limited hydrologic data suggests that fresh groundwater beneath portions of the study site closest to the coast occurs in thin sheets and increases in thickness further from the coast line. Various public and private supply wells have been installed across the study site for irrigation purposes primarily (Farrell *et al.*, 2002) and have been monitored by the BWA staff.

# CHAPTER 2 REVIEW OF LITERATURE

## 2. 1 Convergence of geomorphology and groundwater studies on karst

A wide variety of equations has been used to solve groundwater flow problems including those of saturated/unsaturated flow and of interactions between groundwater and surface-water. These problems can be solved fairly accurately using numerical models as long as the hydraulic parameters, as well as the initial and boundary conditions of the modelled regions are known. However, complications arise in karst terrains as carbonate rocks are soluble in water, i.e., groundwater, and this consequently alters the study region's hydraulic parameters as well as the geology and/or geomorphology. This coincides with the view of Kiraly (2003) that: "karstification or karst evaluation must be undertaken when solving karst hydrology given its influence on the groundwater flow field". Recent two- or three-dimensional numerical groundwater models such as SUTRA (Voss, 2003) or MODFLOW (Harbaugh *et al.*, 2006) are examples of the merging of the sciences of geomorphology and groundwater hydrology. These models have increased one's ability to model landforms of similar morphology and have improved current understanding of groundwater flow systems.

The vulnerability of groundwater to pollution, particularly in karst regions, is another factor that emphasizes the need of including geomorphologic parameters in groundwater modelling. For example, spatial location of pollutants and their relation to sinkholes can be included in modelling processes so as to increase the accuracy of models or delineate the boundaries of protection zones.

The completion of numerous case studies in karst regions has entailed combining knowledge of geomorphology and groundwater: in particular, given their influence over regional hydrologic patterns, the interrelationships between karst surface features and the groundwater borne in underground conduits (Patton and Klein, 1989; Singh, 1989). For example, Patton and Klein (1989), studying the influence of sinkhole formation on the regional hydrology of the Peace River (Polk County, FL), showed that the water-table drawdown in the aquifers was increased under conditions of heightened dissolution and sinkhole collapse. Ryan (1989) simulated groundwater flow between sinkhole lakes and the aquifer along the Central Florida Ridge to investigate the occurrence of leakage through the lake bottom. Such leakage was found to take place when (i) the anisotropy ratio was less than 100, and (ii) the hydraulic gradient was less than 0.02. Chen *et al.* (1995) discussed the effects of the development of karst features on groundwater quality, showing that nitrogen-bearing compounds (i.e., $NO_3^-$ and $NH^{4+}$) in the aquifer tended to disperse along the orientation of major regional fracture lines (e.g., sinkhole alignments). Additionally, rapid vertical flow was found to carry warm surface water into the limestone aquifer, where the karst features present served as local pathways to introduce contamination. These studies show how important it is to consider the geomorphologic characteristics of karst terrains when addressing their groundwater problems.

## 2. 2 Karst geomorphology studies

Only in the past two decades have new initiatives been carried out to improve our understanding of interactions between geomorphologic features and the local ecosystems. This has coincided with increased awareness amongst the public that while our geomorphologic heritage must be preserved, geomorphologic processes hazardous to human life and activity must be addressed in a more informed manner (Marchetti and Rivas, 2001). This is particularly critical and challenging on karstlands, thus attracting a range of investigators from diverse disciplines, seeking to develop a comprehensive understanding of karst dynamics.

Knowledge of karst is rather minimal in the present study of geomorphology, so qualitative descriptions of many karst areas are incomplete due to the chaotic nature of karst (Jennings, 1985). Studies of karst geomorphology have often focused on the surface features since these are the features most easy to be recognized and categorized. Karst landforms, such as sinkholes and fractures, often form recognizable patterns including zonations, lineaments and dendritic networks. According to Kastning (1989), under some circumstances, well established groundwater patterns are expressed on the land surface. Readily identifiable karst surface features, for instance, have been used to interpret underground conditions, that were otherwise hidden from view (Kastning, 1983).

Approaches or methods applied to karst geomorphologic studies have sought to provide substantial insights towards understanding its underground components. Tasks such as mapping, quantification, and interpretation of surface landforms are often essential assessments prior to on-site surveys for environmental or engineering planning (Ogden *et al.*, 1989). These techniques have been employed in various case studies seeking either to quantify karst landforms, or to map out the spatial distribution and patterns of karst features.

### 2. 2. 1 Quantifying karst landforms

Providing important measurements and mathematical analyses modeling of the Earth's surface and its landforms "morphometric techniques" are often used to provide objective and quantitative descriptions of karst landforms (Bates and Jackson, 1987;

Denizman, 2003). These techniques have also been demonstrated to be successful in locating landforms in various karst regions (Day, 1983; Williams, 1972b).

Sinkholes are special features of karst topography which represent one of the most important processes of karst geomorphology (Cvijic, 1957). Because of their importance, they have been used frequently as an index of karst landforms. Quantitative morphometric techniques applied to sinkholes and their density were first introduced by Cramer (1941). Other early uses of morphometric parameters include: (i) the elongation ratio (length/width) to quantify sinkhole shapes (LaValle, 1967); (ii) width, length and depth to differentiate families of landforms (White *et al.*, 1966), (iii) applying the ordering of river basins to sinkholes and stream water basins (Horton, 1945; Strahler, 1957). As discussed by various authors, applying morphometric techniques to sinkholes is a means of quantifying the size, shape, distribution, and hydrogeologic controls on the development of closed depressions in karst terrains (Ford and Williams, 1989; Ogden *et al.*, 1989; Williams, 1972a, 1972b).

Since various morphometric parameters of sinkholes were defined, they have been applied to different karst terrains to provide objective descriptions of karst phenomena, such as the characteristics of sinkhole occurrence. A study on karst sites in Kuwait showed the distribution of cavities and sinkholes to be aligned with local structural fault systems as well as sinkhole axes (Abdullah and Mollah, 1997). Similar distributions were observed among 25,000 sinkholes in the Western Highland Rim of Tennessee and the Pennyroyal Plain of Kentucky (Kemmerly, 1976, 1980 & 1982). While Barlow and Ogden's (1982) study in northwest Arkansas also demonstrated significant specific orientations in sinkhole axes. Another cause of sinkhole occurrence was suggested to be the outcrop of highly soluble relatively flat-lying carbonate stone, resulting in zonations of sinkholes. Such phenomena were observed in central Kentucky (Quinlan, 1970), Western Kentucky (Kastning and Kastning, 1981), and in Indiana as well as wide valley bottoms of the Appalachian Valley and Ridge Province (Hubbard, 1988).

Moreover, sinkhole growth/enlargement has been studied extensively in a number of karstlands. Diane (2000), working in Greenbrier Country, West Virginia, observed that: (i) sinkhole depth increased with increasing length, width and area; (ii) sinkholes tended to become more rounded with increases in their width, area and depth; (iii) sinkhole length, width and area were proportional to one another, but increased at different rates; (iv) larger sinkholes formed in pure limestone containing less clay; (v) sinkhole orientation was correlated with regional lineaments. Moore (1976, 1981 & 1987) argued that highway construction had effects on sinkhole development based on his studies conducted in East Tennessee, Additionally, certain karst structures were found to contribute to sinkhole enlargement (e.g., LaValle, 1967; Kemmerly, 1976; Ogden & Reger, 1977; Soto and Morales, 1984; Littlefield *et al.*, 1984; Nelson, 1988). Another important factor indirectly associated with sinkhole enlargement is bedding thickness which controls the rate of fracture dissolution (Dreiss, 1984; Kastning, 1975; Palmer, 1962; Rauch and White, 1970). Thinly bedded limestone was found to undergo greater dissolution and mechanical breakdown of conduit roofs, resulting in larger conduit openings (i.e., sinkholes).

Furthermore, numerous morphomeric analyses of karst surface features have been extensively applied in an attempt to predict underground conditions. Odgen and Reger (1977), attempting to predict ground subsidence in Monroe County, West Virginia, showed that the percent area covered by sinkholes could be used as an index of subsidence risk. Similarly, in Cookeville, in the Eastern Highland Rim Province of

Central Tennessee, sinkhole morphometry was used to predict sinkhole flooding. The sinkhole alignment/lineaments were used to infer underground faults as well as to provide information on the extent of underground drainage basins or patterns of groundwater flow.

As described, the geometric characteristics of sinkholes are of major interest in the quantification of karst landforms. Applying morphometric analysis on sinkholes has been shown to provide objective descriptions of karstlands and provide a valuable means of understanding underground conditions.

### 2. 2. 2 Spatial distributions and patterns of karst features

The most common approaches and methods for studying karst distribution patterns were first developed by plant ecologists and extended by geographers (Ford and Williams, 1989). Investigations on the spatial distributions and patterns of karst features have often focused on the spatial appearances of sinkholes, which can occur as scattered isolated individuals, as scattered clusters of individuals, as densely packed groups, or as irregularly spaced chains along dry valley systems (Ford and Williams, 1989). Sinkhole density and sinkhole nearest-neighbours have been widely discussed and used as indications of sinkhole spatial distributions and patterns (White, 1988).

White and White (1979), working in the Appalachians regins, defined sinkhole density as the total number of sinkholes divided per unit area, a parameter which has frequently been applied to karst areas as an index of karstification. Similarly, Shofner *et al.* (2001), also working in Tennessee, introduced an easily determined index of surface karstification, termed 'sinkhole index', based on the main spacing of closed contours in a given area. This index showed a high correlation with total sinkhole area and a moderate correlation with total sinkhole volume. However, the relationship between caves and sinkhole distribution was poor. Furthermore, sinkhole density has been extensively used to produce the karst hazards maps, such as those developed by Miller (1977) for an area in Tennessee. The maps were constructed based on the identification of areas with a high density of karst features and specific types of bedrock geology. Bahtuarevic (1989) conducted a comparable study to produce a sinkhole density map of 385 sinkholes in the Forest City Quadrangle of Central Florida. This map was used to evaluate applications for sinkhole hazard prediction, and was further extended to construct sinkhole-risk models used in sinkhole risk assessment. Gao and Alexander (2001) constructed a sinkhole probability map for Goodhue County, in south-eastern Minnesota, based on sinkhole distribution, bedrock geology, depth to bedrock, and nearest-neighbour analysis.

Pattern analysis uses the term "intensity" to describe the type of density encountered in different locations, and intensity patterns have been used to describe sinkhole distribution phenomena. In 1954, Clark & Evans developed an analytical method called "Nearest neighbour analysis" to determine distribution patterns of sinkholes. This method has been applying in various karst terrain investigations (Williams, 1972a and 1972b; Day, 1978, 1983; Gao and Alexander, 2001; Denizman, 2003). Table 2-1 presents a demonstration of nearest neighbour analysis as applied to the karst regions of such Caribbean islands as Barbados, Antigua, Guadeloupe, Jamaica, and Puerto Rico. A nearest neighbour index ($\overline{R}$) was obtained by dividing the mean actual distance between neighbouring sinkholes in a karst region to the mean expected distance between neighbouring sinkholes. $\overline{R}$ value varies from 0 for dispersion with maximum aggregation or clustering, through 1 for a random case, and to 2.149 for a regular pattern.

**Table 2-1:** Sinkhole density and nearest neighbour statistics for several karst regions on the Caribbean islands (Day, 1978)

| Region | Sinkhole density ($km^{-2}$) | $\overline{R}$ | Pattern |
|---|---|---|---|
| Barbados | 3.5-13.9 | 0.874 | Tending to cluster |
| Antigua | 0.39 | 0.533 | Clustered |
| Guadeloupe | 11.2 | 1.154 | Near random |
| Jamaica (Browns Town-Walderston Formation) | 12.5 | 1.246 | Approaching uniform |
| Jamaica (Swanswick Fm.) | 12.4 | 1.275 | Approaching uniform |
| Puerto Rico (Lares Fm.) | 15.3 | 1.141 | Near random |
| Puerto Rico (Aguada Fm.) | 8.7 | 1.124 | Near random |

$\overline{R}$ : Nearest neighbour index

Gao (2002) suggested that sinkhole clustering occurs because such zones had similar geologic and topographic characteristics favouring sinkholes formation. Additionally, the existing sinkholes affecting the hydraulic gradient in the surrounding area increased the dissolution and erosional processes and led to the formation of new sinkholes. Karst geomorphology and groundwater dynamics can be illustrated by multiple correlations between karst surface phenomena and sub-surface mechanisms (Figure 2-1).

Investigators of karst landscapes have been trying hard to predict underground environments by interpreting surface patterns (Mills & Starnes, 1983; Ford, 1984). In many cases, less expensive surface interpretation is the only practical way of obtaining data since time and cost constraints usually limit the amount of expensive subsurface exploration possible. Interpretation of surface karst features has frequently been incorporated in the assessment of land-use management, construction, groundwater determinations, waste disposal, etc. In this case it is sufficient and common to interpret surface ground features from sources like aerial photographs and topographic maps. Yet, Kastning (1989) suggested that for accurate conclusions to be drawn, on-site fieldwork, tracer studies and some physical techniques must be employed.

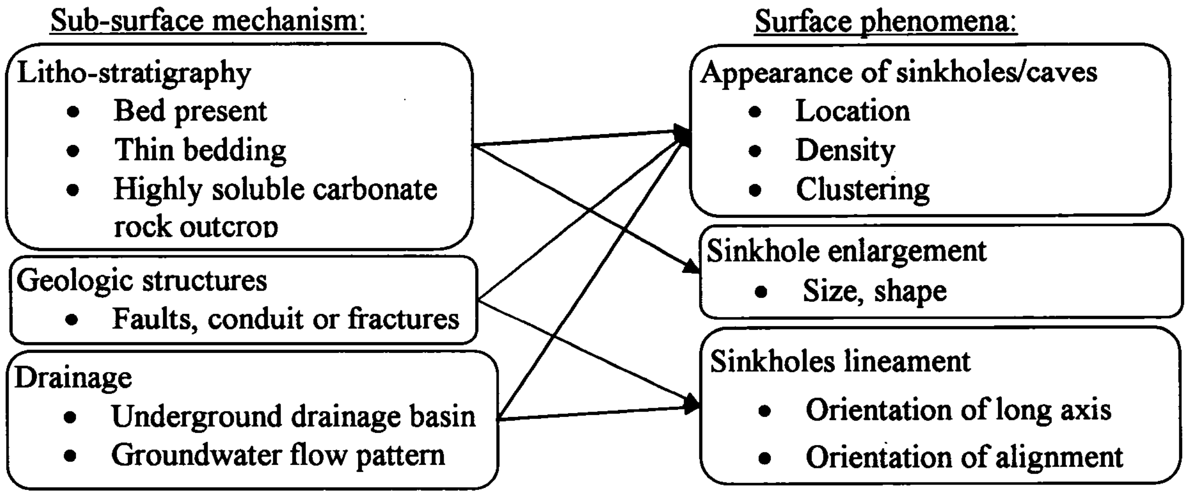


**Figure 2-1:** Correlations between karst surface phenomena and sub-surface mechanisms

## 2. 3 Overviews of previous Barbados geomorphologic studies

The geomorphologic studies on the island of Barbados have mainly appeared in the European literature. In Coleman and Balchin's (1959) study, Barbados was taken as a test case for the general model of karstification they proposed. They assumed Barbados karst to represent an early stage of valley cutting followed by desiccation linked to increasing drainage and sinkholes. The sinkholes investigated were identified on 1:10,000 topographic maps with a 6-m contour interval based on the highest closed contours. These sinkholes were found to enlarge with age. The number of sinkholes counted was reported to be under-estimated due to difficulties in measuring small and shallow sinkholes accurately with a planimeter. Nevertheless, Coleman & Balchin (1959) concluded that Barbados valleys were cut following intense rains, with high slopes as an added influence in favour of run-off. Karstification of these valleys was only a partial and secondary cause of their desiccation. The varied valley density over the Coral Cap was related to differences in the frequency of intense rains today.

Fermor (1972) studied the pattern and origin of karstic features in the island of Barbados by reviewing various studies conducted on the island. Under his approach sinkholes were usually discrete, predominantly circular in form and seldom greater than 15 m in depth. The valleys were frequently incised to depths of 39 m and their sides commonly sloping by over 30° and rarely less than 15°. The pattern of these valleys was pinnate with some trellising.

A comprehensive investigation of sinkhole morphology and development in northern Barbados (St. Peter, St. James, and parts of St. Lucy and St. Thomas parishes) was conducted by Day (1983). Some 1179 sinkholes were identified from 1:10,000 scale aerial photographs (1964), and 360 were surveyed within a total area of 124.4 $km^2$. His results showed the development of sinkholes and dry valleys to be competitive, particularly in the western part of the island. He also observed sinkhole density to increase with altitude up to 150 m, but to decline thereafter. The spatial distribution he observed indicated a tendency of clustering, but there was little evidence of structural controls producing preferred long-axis orientations. Like Coleman & Balchin (1959), Day (1983) encountered difficulties in identifying karst features from aerial photography due to their being obscured by dense vegetation. He had concluded there to be a miscounting on small (<5 m diam.) sinkholes. As with Day (1983), Wandelt (2000) identified sinkholes across the entire island of Barbados using 1:10,000 aerial photography taken in 2000, measured the size of sinkholes by on-land surveying, to produce a map showing the karst surface features of Barbados.

Unlike other geomorphologic studies conducted on the island of Barbados, Jones (2003) developed a study of climate influences on tropical karst. His major interests were focused on the hydrogeologic and climatic influences on spatial and inter-annual variation of recharge in Barbados' karst aquifer. He concluded that karst shafts had greater potential to recharge the aquifer as conduits than the larger inter-fluvial sinkholes characterized by low soil permeability. He further proposed that karst shafts occurring on the sides of dry valleys can potentially transmit large volumes of water to the aquifer during brief periods of runoff ( Jones *et al.*, 2000; Jones, 2003). Based on the seasonal fluctuations in rainwater $\delta_{18}O$ (the ratio of stable isotopes) values, Jones *et al.* (2000) showed that greater recharge rates occurred at lower elevations in response to discrete infiltration of large volumes of water through the highly permeable limestone. Moreover, he proposed that groundwater flow paths in this aquifer were controlled by the topography of the top of the aquitard.

### 2. 4 Acquisition of karst morphometric data

#### 2. 4. 1 Topographic maps

It has been proven that the most accurate method to obtain data for morphometric analysis is from detailed field topographic surveys (Ford and Williams, 1989; Jennings, 1975); however, this procedure is costly, time consuming, and only allows the coverage of a small area. More often than not, morphometric data are obtained from topographic maps; however, the sufficiency and accuracy of such results are strongly influenced by the dimensions of features, the scale of the map, the contour interval, and the slope of the ground surface around the features (Ford and Williams, 1989). For example, Day (1983) in locating sinkholes on Barbados from 1:10,000 scale maps, found that he underestimated the numbers of sinkholes by up to 54%, when compared to field surveys. As discussed by Ford and Williams (1989) the major problem with acquiring earth features from maps is their variable quality and density of information.

### 2. 4. 2 Photogrammetry

Photogrammetry has been widely exploited in geomorphology. The use of aerial photographs by geomorphologists, for example, has included both qualitative analysis of landforms and recovery of quantitative information by conventional analogue photogrammetry (Lane *et al.*, 1996). While some special difficulties have been discussed when applying photogrammetry to karst regions (Jennings, 1985; Ford and Williams, 1989), viewing large scale stereoscopic aerial photographs has proven generally preferable to topographic maps in terms of acquiring morphometric data. However, heavy forest cover or shadows could result in masking hydrographic and topographic details. Compared to other landscape types, intensive ground checking is particularly important for karst landscapes.

### 2. 4. 3 Digital elevation models (DEMs)

Apart from traditional methods, significant improvement on the availability of producing digital elevation models (DEMs) has increased the possibility of measuring and monitoring terrain spatially in three dimensions. DEMs, traditionally derived from contours or ground surveys, are in raster format, storing one elevation value per pixel, thus representing actual areas in the real world. Recent enhancements in the technologies of remote sensing and image-processing have made it possible to acquire DEMs by triangulating from stereo-pairs satellite imagey, i.e., SPOP, IRS, ASTER, and LIDAR (Chirico, 2004). The critical issue in obtaining confident results from DEMs is their resolution. Chenoweth (2003) developed a bio-geomorphologic database based on satellite imagery (ASTER) derived DEMs to classify and quantify karst landforms and associated vegetation densities in Jamaica's Cockpit country. He reported that satellite imagery acquired in wet/dry seasons at a high resolution (< 4 m) increased the capacity for landform identification.

### 2. 4. 4 Remote-sensed imagery

Besides extracting DEMs from stereoscopic satellite imagery, processing multi-spectral imagery also provides quick and useful baseline information of geology, lithology, structure, geomorphology, soils, landuse/cover, lineaments, etc. Chen (1992) used LANDSAT multi-spectral scanner and thematic mapper imagery to define and delineate regional landforms, drainage basins, and lithological units. Image processing was based on tones/colors, textures, drainage patterns, and topographic expression. Similarly, Dimadi and Tsakiri-Strati (2004) integrated the use of thematic mapper imagery, digital terrain model and 3D visualization in groundwater studies on karstified marbles in Turkey.

## 2. 5 Applying GIS technologies on karst geomorphology

Rapid achievements in computer technology have revolutionized the way we communicate and visualize the results of our work, in particular the realizations of Geographic Information System (GIS). Although GIS applications have been used in environmental management for decades, the use of GIS to study karst is a relatively new and rapidly growing domain (Szukalski, 2002). GIS is a science combing geographic information and multidisciplinary technologies which increase the efficiency and effectiveness of managing land resources. ESRI (2005) defined it as a system for management, analysis, and display of geographic knowledge using a series of information sets, such as maps and globes, geographic data sets, processing and work-flow models. Its applications have been widely used in hydrology and geomorphology to automate basin, hill-slope, and stream network analyses. Several commercial GIS applications and softwares have incorporated the more common terrain attributes (e.g., slope, aspect, and curvature) and terrain analysis procedures (e.g., basin and stream network extraction) (Lindsay, 2004). Common uses of GIS in karst geomorphologic studies are visualizing landforms, managing geospatial databases, and conducting spatial analyses.

### 2. 5. 1 Visualizing landforms

According to Phelan (2002), the spatial modeling and visualization capabilities of GIS provide the most effective means to convey complex spatial relationships to the human mind. When trying to model land-surface and subsurface hydrogeologic linkages, the inherent complexity of environmental processes is compounded, since these processes are often hidden from view and are thus, more difficult to comprehend or verify. This is the main reason that GIS applications are increasingly used to develop conceptual models from sparse information, particularly in karst terrains. Organizations and agencies in Kentucky, for example, have developed extensive databases providing a wide coverage of geographic features in the US (Florea and Paylor, 2002). The commercial GIS software, ESRI ArcView, was employed by Florea and Paylor (2002) to conduct a 3-D modelling of the Hidden River Cave System in Horse Cave, Kentucky. Digital Line Graph (DLG), Digital Ortho Quarter Quad (DOQQ) data and cave survey data were incorporated to display the relationships between the sub-surface conduits, topography and town of Horse Cave. Other examples can be found in the research of Phelan (2002) who constructed a 3-D visualization of the subsurface of a karst terrain based on public domain water well drilling logs. A 3-D visualization model of subsurface displacements was constructed to investigate the correlations with surface topography obtained from DEMs. He concluded that a 3-D model can improve the effectiveness of limited funding by using public datasets, contribute to the development of conceptual hydrogeologic models, and locate areas meriting additional investigation.

### 2. 5. 2 Managing geospatial database

Besides their visualization capability, the database management systems of GIS have been widely used to develop karst feature databases for spatial manipulation and resource management (Whitman and Gubbels, 1999). Various studies have implemented a karst database to enhance data accessibility and resource management across countries (Cooper *et al.*, 2001; Lei *et al.*, 2001). Especially in the United States, karst inventories have been established across the country (Gao *et al.*, 2002; Whitman & Gubbels, 1999), and series of karst maps have been produced (Veni, 2002). Specific achievements such as developed a comprehensive Karst Feature Database (KFD) of Minnesota (Gao *et al.*, 2002) used GIS to document 11,682 karst features. Green *et al.* (2002) inventoried karst features, e.g., sinkholes, streams, caves, dry valleys, and springs in Mower County, south-eastern Minnesota. A GIS-based karst unit map was also developed using bedrock type, depth to bedrock, topography, surface and subsurface hydrology, spring chemistry, etc (Green *et al.*, 2002). This map was used to interpret karst hydrologic systems for further decision-making on feedlots, quarries, housing developments, and landfills. Furthermore, an integration of a GIS-based database with the groundwater model MODFLOW was evaluated by Brodie (1998), based on borehole information in the Murray Geological Basin, southeast Australia.

### 2. 5. 3 Conducting spatial analysis

Above all, the GIS analytical functionalities provide powerful tools to help to understand the distribution of spatial features and model their interactions, i.e., finding previously unrecognized patterns and relationships. Denizman (2003) demonstrated an application of GIS to examine the morphometric and spatial distribution of 25,000 sinkholes in the Lower Suwannee River basin. The calculations of morphometric parametersI included length, width, orientation, area, depth, circularity index, sinkhole density, pitting index, and nearest neighbour index. Additionally, GIS applications have advanced the management of karst collapse in China, including the development of a national collapse inventory and the performance of risk assessments of potential karst collapse (Lei *et al.*, 2001). As a result, 1,446 karst collapse events and 45,037 sinkholes were documented and analyzed using GIS.

## 2. 6 Alternative strategies to manage karst lands

Acknowledging karst as a complex system and focusing efforts on protecting the integrity of karst systems and individual karst features are key elements to karst resource management. As karst is not as systematic as other types of terrains, physical laws applicable in general to other landforms cannot be applied to karst. In most cases, the formulas must be modified to respond to local causes, specific parameters and human activities in order to describe a specific karst landform. Apart from characterizing karst terrains, developing efficient management strategies is also essential for better exploitation of karst resources.

The identification of geomorphologic assets is an important approach leading to successful management of vast karstic resources. According to Marchetti and Rivas

(2001), methods for identifying and evaluating geomorphologic assets on a scientific basis are subdivided into two phases: (i) geomorphologic survey and mapping, and (ii) selection from geomorphologic maps of those landforms that may be considered as assets. When particular karst landforms are identified, the vulnerability of karst terrain should be carefully inventoried and assessed for proposed developments. The "*Karst Inventory Standards and Vulnerability Assessment Procedures for British Columbia*" (2001), published by the Ministry of Forestry in the province of British Columbia (Canada), is an inclusive guideline for conducting karst inventories and vulnerability assessments. This report describes and suggests required data collection and evaluation for three levels of inventory to assist best strategic/resources planning on karst. Based on the resulting karst vulnerability assessment, the "*Karst Management Handbook of British Columbia*" (2003) was then followed to select best management practices designed to sustain forest practices on karst landscapes and minimize impacts to timber supply and operational costs. Significant karst features including cave entrances, above caves, surface karst features, karst springs, and unique or unusual karst flora/fauna habitats that should be protected by reserves. This handbook gives appropriate sizes and shapes for such reserves, according to the conditions of the site, e.g., slope.

Furthermore, Elhatip (1997) suggested that karst aquifers, springs, sinkholes, poljes and other karst features are of great importance for conserving and protecting groundwater resources for both qualitative and quantitative standpoints. A conventional approach used in protecting karstic aquifers is the defining of groundwater protection zones, such as described by Singh (1989). He proposed that industrial and municipal effluents should not be disposed of around sinkholes to prevent pollutants being carried to groundwater through an intricate network of interconnected sinkholes. However, Doerfliger *et al.* (1999) argued that defined groundwater protection zones in karst environments are frequently not founded on a solid hydrogeological basis, and may lead to ineffective results. He proposed that groundwater protection zones should be based on the vulnerability mapping of the catchment area of water supplies from springs or boreholes. His vulnerability mapping was defined by the intrinsic geological and hydrogeological characteristics. Factors such as type of karst, protective cover, infiltration condition, and karst network development would affect sensitivity of groundwater to contamination. This method was applied to several sites in Switzerland with agriculture contamination problems to define boundaries of protection zones for safer karst water supplies.

Finally, the involvement of local policy/decision-makers is important in managing karstlands, since the environmental issues in karstified areas are often diverse and encompasses local, regional, and global problems. Management impacts on water quality and quantity are particularly of interest from a human and financial point of view. LaMoreaux *et al.* (1997) documented a series of publications associated with environmental and legal aspects of karst, in particular some correlative developments of international laws and global agreements on karst water. As described in the document, the regulatory standards for karst in the United States have progressed to maturity, as karst aquifers are a major resource of drinking water there (providing $2.5 \times 10^7$ $m^3$ $day^{-1}$ in 1985). The major karst aquifers across the United States have been studied in detail, including critical information on the topography, geology, hydrology, climate, and land used. Various federal laws (e.g., Clean Water Act) concerning groundwater in karst areas have been developed in order to standardize water withdrawals, and protect water quality from agricultural or industrial developments.

# CHAPTER 3 METHODOLOGY

## 3. 1 Data acquisition

### 3. 1. 1 Identification of parameters

A database structure (Appendix C) developed for conceptual groundwater modelling was implemented. This database structure was obtained from the Standard Guide for Conceptualization and Characterization of Groundwater Systems (ASTM, 2002) and served as a systematic guideline for data acquisition. While 11 parameter categories were included in the guide, the categories related to the geomorphologic characteristics of landforms were those of major interest for this study. Consequently, data on parameters such as climatic conditions, vegetation and soil types were not collected.

### 3. 1. 2 Data gathering and assembling

From September to December 2004, various data associated with the identified parameters were assembled (Table 3-1), and classified into five categories: geomorphology, hydrology, anthropogenic aspects, geology, and remote-sensed imagery. Details of the data collected are described in the following sections.

**Table 3-1:** Data collected in the study

| Data Category | Data Type | Source | Year | Scale | Format | Grid** |
|---|---|---|---|---|---|---|
| Geomorphology | Topography (10 ft) | Lands & Surveys Department | 1977 | 1: 2500 | Cartography | BWI |
| | Topographic contours (10 m) | Barbados Water Authority | Unknown | 1: 10,000 | ArcGIS (*.shp) | BNG |
| | Bathymetry | Coastal Zone Management Unit | 2000 | 1: 10,000 | AutoCad (*.dwg) | WGS 84 UTM |
| | Geology – elevation of coral base | Barbados Water Authority | 1981 | 1: 10,000 | Cartography | BWI |
| Hydrology and lithology | Shoreline | GeoCaribe Ltc | Unknown | 1: 10,000 | ArcGIS (*.shp) | BNG |
| | Borehole | Barbados Water Authority | Unknown | N/A | EXCEL (*.xls) | BWI |
| | Groundwater catchments | Barbados Water Authority | Unknown | N/A | ArcGIS (*.shp) | BNG |
| | Lithology | Barbados Water Authority | 2004 | N/A | EXCEL (*.xls) | BNG |
| Anthropogenic aspects | Roads | GeoCaribe Ltc | 2004 | 1:10,000 | ArcGIS (*.shp) | BNG |
| | Buildings | GeoCaribe Ltc | 2004 | 1:10,000 | ArcGIS (*.shp) | BNG |
| | Groundwater protection zones | Barbados Water Authority | Unknown | N/A | ArcGIS (*.shp) | BNG |
| Geology | Surface geology | McGill Univ. Library | 1983 | 1: 50,000 | Cartography | BNG |
| Remote-sensed imagery | LIDAR (Light Detection and Ranging) -31 cm | Coastal Zone Management Unit | 2000 | N/A | *.SID | WGS 84 UTM |

**Grid: the details of the grid system used in the collected data were described in pages 43 and 44.

#### 3. 1. 2. 1 Geomorphology

**Topographic maps (contour interval: 10 ft):**

Thirteen 1:2,500 scale topographic quadrangles (10-ft contour intervals) were provided by the Lands and Surveys Department (Figure 3-1a) of Barbados government. These maps, (29NE, 29SE, 30NW, 30SW, 30NE, 30SE, 31NW, 31SW, 37NE, 38NW, 39NW and 39NE), based on aerial photography and field surveys undertaken in 1977, were produced by the British Government's Ministry of Overseas Development. The importance of these maps was their relatively small contour interval (10 ft, i.e., ≈3.3 m) and was the most detailed available allowing one to locate surface features, i.e., sinkholes and gullies. Their contours were digitized and used to delineate the surface DEM of the study area. These 13 maps (the only such data available) cover 70 % of Porters and Trents catchments (leaving the upper 30 % not covered). Thus this study was restricted to the map area actually covered (Figure 3-1b).

**Geology – elevation of coral base**

Two 1:10,000 geologic quadrangle maps (Figure 3-2) containing elevations (referenced to mean sea level) of the coral base (10 m - interval) beneath the study area were provided by the Barbados Water Authority. The elevation information was used to locate the boundary between the coral rock and the underlying oceanics, and to generate a subsurface DEM of this boundary.

**Digital contours (10 m interval)**

One 1:10,000 scale 10-m contour digital file of the entire island of Barbados was obtained from the Barbados Water Authority. The map was initially digitized from topographic quadrangle maps by the BWA staff and stored in ESRI shapefile format.

**Bathymetry**

The bathymetry data were obtained in digital AutoCad format (*.dwg) from Barbados Coast Zone Management Unit. The 1:10,000 scale bathymetry maps were originally produced by an Airborne Scanning Laser Bathymetry System, and were referenced to mean sea level. The elevation range of the bathymetry was from 0 to -45 m (Figure 3-3). These data were combined with inland surface contours extracted from the 1: 2,500 scale topographic maps to produce a continuous surface DEM.

**3. 1. 2. 2 Hydrology and lithology:**

Hydrologic data included shoreline boundary, locations of boreholes/drill wells and boundaries of groundwater catchments. Lithologic records were extracted by the BWA from monitored borehole/drill wells (see Appendix D) and were used to verify the depths of the coral base beneath the study area as obtained from the 1:10,000 geologic maps.

**3. 1. 2. 3 Anthropogenic aspects**

A digital road network map and buildings map digitized from recent aerial photography and high-resolution satellite imagery were provided by GeoCaribe, a private GIS-data company. The road network in the study area was updated based on two LIDAR images (2003). A digital file containing the groundwater protection zones of the island (Figure 1-7) was provided from BWA. Detailed descriptions of the defined zones are given in Appendix A.

### 3. 1. 2. 4 Surface geology

One 1:50,000 scale surface geology map of Barbados produced in 1983 by the British Government's Ministry of Overseas Development was obtained from the Walter Hitschfeld Geographic Information Centre of McGill University. Surface geologic boundaries were digitized to study hydrogeological influences on karst landforms.

### 3. 1. 2. 5 Remote-sensed imagery

Two images obtained using LIDAR (Light Detection and Ranging) technology and covering the study area were provided by the Barbados Coastal Management Unit. High resolution LIDAR images (0.31-m resolution) enabled the pre-location of karst surface features and facilitated the process of field investigations, especially when attempting to identify surface features across large landscapes.

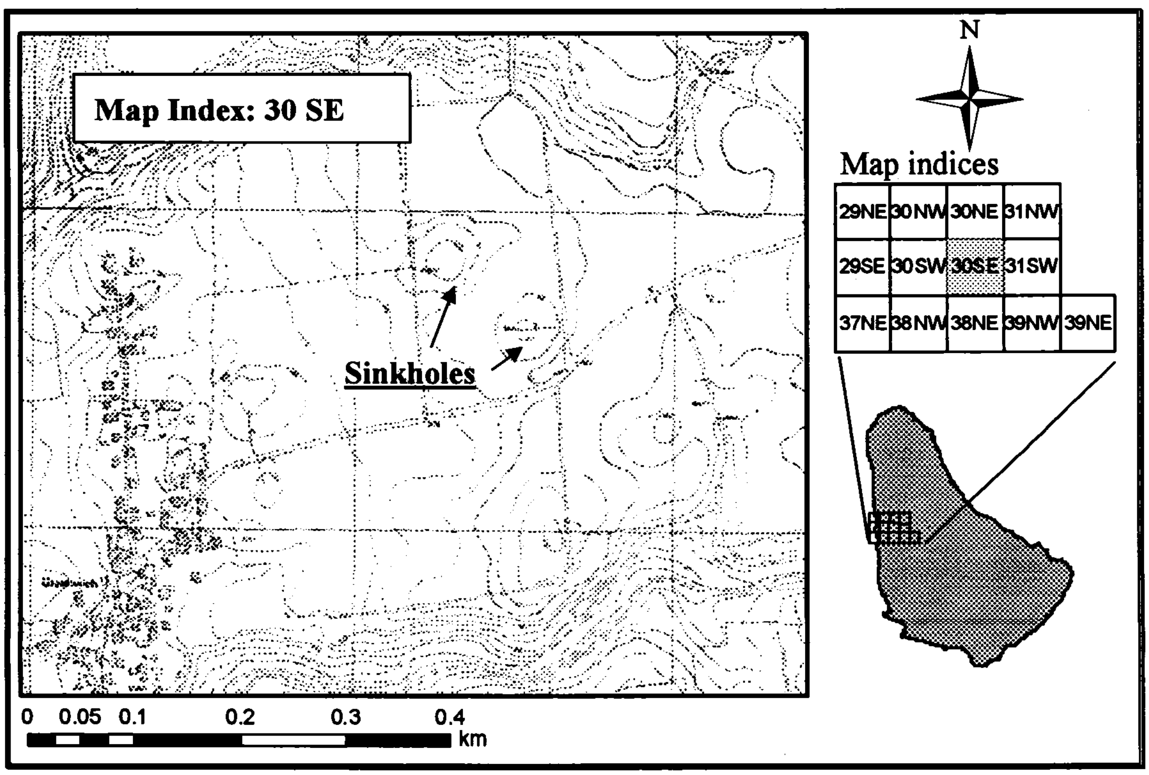


**Figure 3-1a:** The 1: 2,500 scale topographic quadrangle maps.

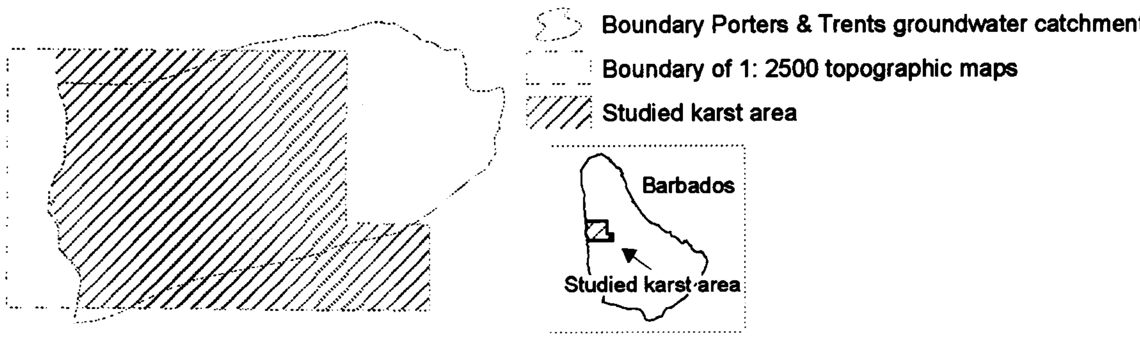


**Figure 3-1b:** The studied karst area covered by 1: 2,500 scale topographic maps.

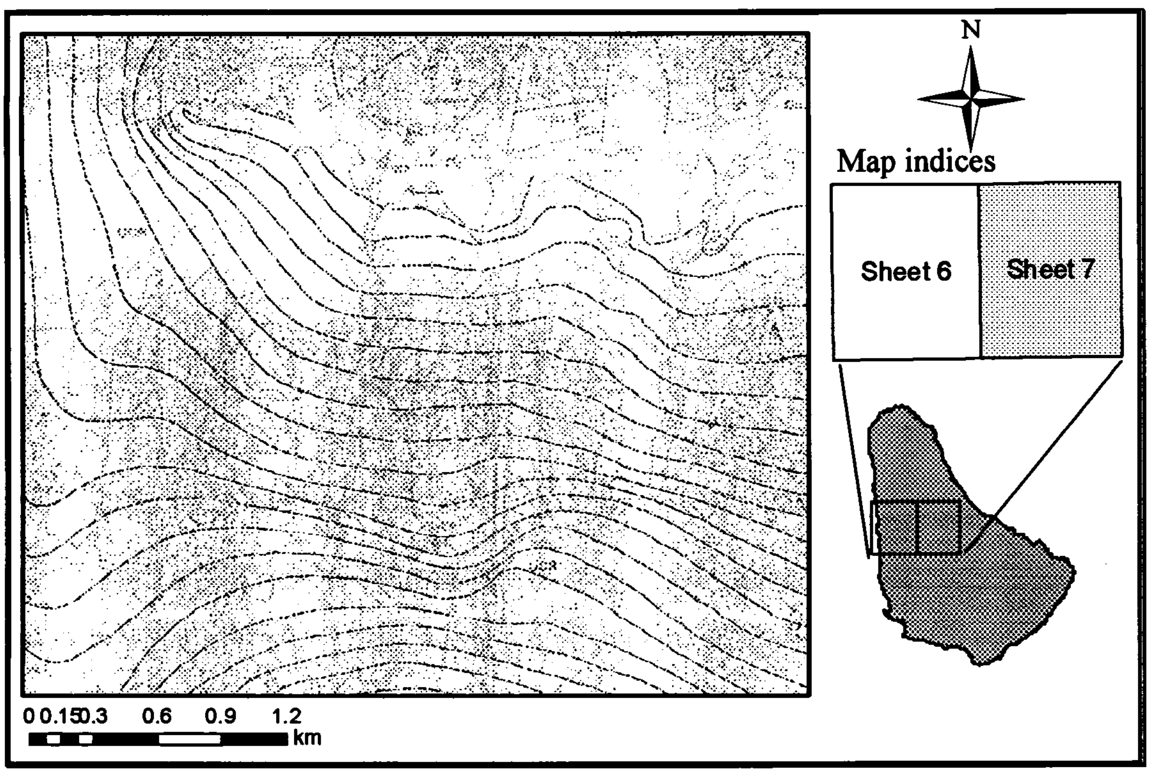


**Figure 3-2:** The geologic quadrangles showing the elevation of the coral base.

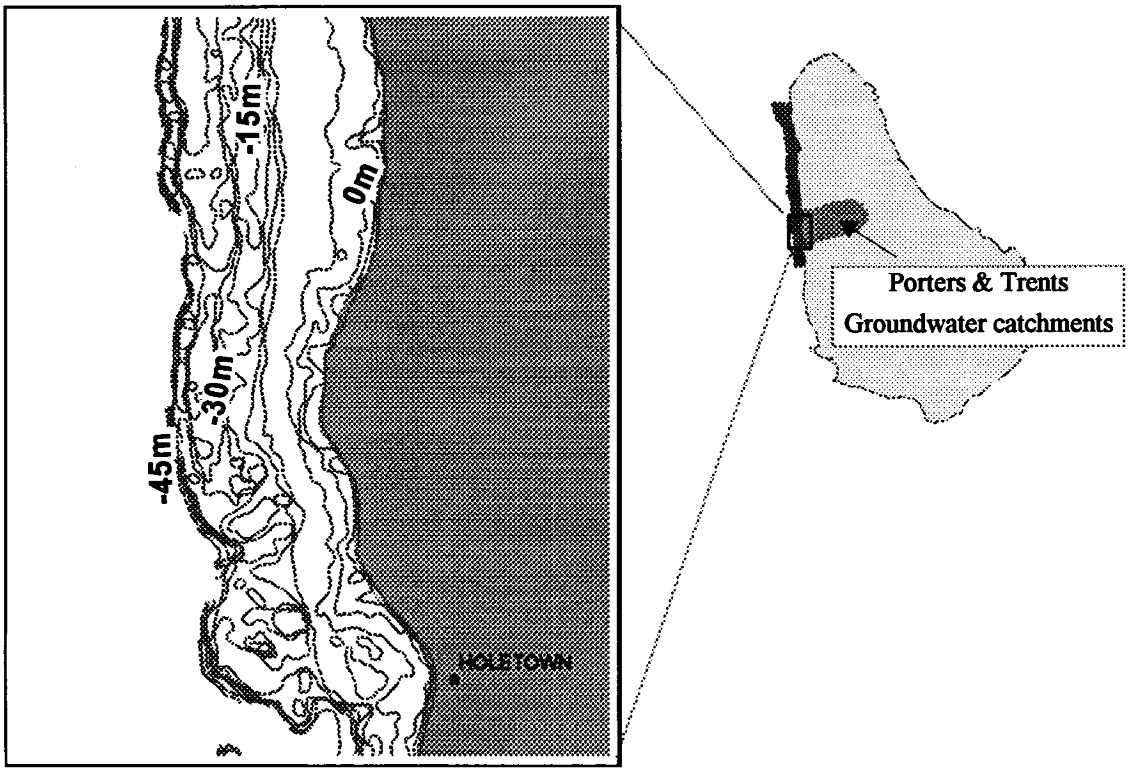


**Figure 3-3:** Bathymetry map along the coast of the study area

### 3. 1. 3 Field observation and verification

Field investigations were conducted to verify the geographic coordinates and obtain conditions of karst surface features, especially sinkholes and gullies. The 1:2,500 topographic quadrangle maps and the 2003 LIDAR images were used to assist in searching for essential features across large areas, especially those covered by abundant vegetation.

Two global positioning system (GPS) units (TrimbleDX4000, Trimble Navigation Ltd., Mansfield) were employed to obtaine geographic coordinates of each identified karstic feature. One unit was set up as a base station at a fixed location; the other one as a rover to collect data in the field. Data received from the rover GPS, in combination with those obtained from the base GPS allowed one to perform differential corrections using the Trimble Pathfinder Office Software Kit. According to the instrument manual this post-processing should lead to an accuracy of less than 1.0 m. A GPS data point was taken at each sinkhole. Data were recorded in the World Geodetic System 1984 (WGS 84) with reference to mean sea level. Besides position acquisition, one or several digital camera images were taken (Figure 3-4) to show the general setting and characteristics of each sinkhole. One scene (Figure 3-4a) shows a sinkhole over which a pond is located and which is surrounded by dense vegetation. The pond suggests a high water-table level. Figure 3-4b shows one of many sinkholes areas which are being cultivated. This could be a potential direct source of agrochemical pollution to connecting aquifers.


(a)
(b)

**Figure 3-4:** Examples of two sinkholes within the study site. (a) rich vegetation covering a sinkhole; (b) surroundings of a sinkhole used as a farm-land.

## 3. 2 Karst database development

### 3. 2. 1 Applications used and system environment

The karst database and geospatial data developed from the information collected for the study area were constructed using GIS applications developed by ESRI (Environmental Systems Research Institute, Redlands, USA). The primary applications used in the study were ESRI ArcGIS 9.0 (ArcInfo license) and ESRI ArcGIS extensions: Spatial Analyst and 3D Analyst

These applications allowed an open GIS environment where generic binary data are imaged in various formats. Additionally, customized programming or tools could be applied to the data resources. In the case of this study, GPS information, remote-sensed imagery, DEMs and various cartographic maps were integrated into a geospatial database. It was important to have all these electronic data resources projected in the same coordinate system so that spatial relationships would be consistent. Geographic transformations between different projections (or grids) were accomplished using the functionalities provided by ArcGIS.

Under the framework of ArcGIS, the two ArcGIS extensions Spatial Analyst and 3D Analyst are essential to produce raster data from vector data as well as other terrain analysis. The extensions served to:

1) produce DEMs from topographic contours,

2) convert feature themes (points, line, or polygon) to grid themes,

3) construct 3D views using DEM and other feature layers.

### 3. 2. 2 Spatial data transformation

#### 3. 2. 2. 1 Digitizing and data preparation

Digitizing was used to transform cartographic information into a digital format. The maps used in the study were scanned and imported into ArcGIS 9.0 as images (*.tiff) and then geo-referenced in order to orient the digitized features. The geographic features (i.e., contours lines, marked with elevation spots, etc.) were traced using a mouse and stored as vector files (or thematic layers) for specific features. The coordinate system of each file was based on the information indicated on the original cartographic map.

Location of boreholes and bench marks obtained from tabulated documents were transformed into geospatial data according to the geographic coordinates accompanying the data records.

#### 3. 2. 2. 2 Map projection transformations

Because sets of geographic data from several sources were compiled in the study, three types of coordinate systems: Barbados West Indies Grid (BWI), Barbados National Grid (BNG), and Universal Transverse Mercator (WGS 84 UTM Zone 21N) were involved (Table 3-2). To correctly overlay different thematic layers or perform spatial operations, i.e., DEM generation, it was essential to produce all geospatial data in the same projection system.

The differences in the datum of projections are the main challenge of projection transformation. As listed in Table 3-2, the datum of UTM WGS 84 Zone 21N is WGS 1984, which is different from either BWI or BNG. No special geographic transformation is required when converting BWI to BNG (or vice versa) as both use the same type of datum. On the other hand, a geographic transformation should be carried out when converting BWI or BNG to UTM. In this study, the Molodensky method (ESRI, 2005) of geographic transformation was applied to perform datum transformations of this nature using ArcGIS 9.0. The designed parameters of this method are three shifts ($\Delta x$, $\Delta y$, $\Delta z$) and the differences between the semi-major axes ($\Delta a$) and the flattening ($\Delta f$) of the two spheroids. The values adopted for the required parameters were: $\Delta x = 32.744$, $\Delta y = 300.307$, $\Delta z = 419.193$, $\Delta a = - 112.145$, and $\Delta f = - 0.54750714$; these parameters were obtained based on one point observation.

**Table 3-2:** Projection systems used in the data of the study.

| Grid Name | BWI (Barbados West Indies) | BNG (Barbados National Grid) | UTM WGS84 Zone 21N |
|---|---|---|---|
| Projection | Transverse Mercator | Transverse Mercator | Transverse Mercator |
| Spheroid | Clarke 1880 (RGS) | Clarke 1880 (RGS) | WGS 1984 |
| Semi-Major Axis | 6,378,249.145 | 6,378,249.145 | 6378137 |
| Flattening | 1/293.465 | 1/293.465 | 1/298.257223563 |
| Unit of Measure | Meter | Meter | Meter |
| Meridian of Origin | 62° W. of Greenwich | 59°33'35" W. of Greenwich | 57° W. of Greenwich |
| Scale Factor at Origin | 0.9995 | 0.9999986 | 0.9996 |
| False Coordinates of Origin | 400000m E. Nil meters N. | 30000 m E. 75000 m N | 500000 m E |
| Datum Name | Barbados 1938 | | WGS 1984 |
| Convergence - Grid | 33'48" | <2° | |

### 3. 3 Spatial operations in a GIS environment

ESRI's ArcGIS applications were used in the study to manipulate the geospatial data of the study area, including deriving new information from existing data, analyzing spatial relationships, and building spatial models. The spatial operations on constructed geospatial data were vector and raster operations.

### 3. 3. 1 Vector operations

Vectors constitute a coordinate-based data model that represents geographic features as points, lines, and polygons (Figure 3-5). When a thematic layer is constructed, a set of advanced analytical vector operations such as analysing pattern, mapping clusters, and measuring geographic distributions can be used. These functionalities were used to perform geometric calculation, distribution pattern, orientation and nearest neighbour analysis.

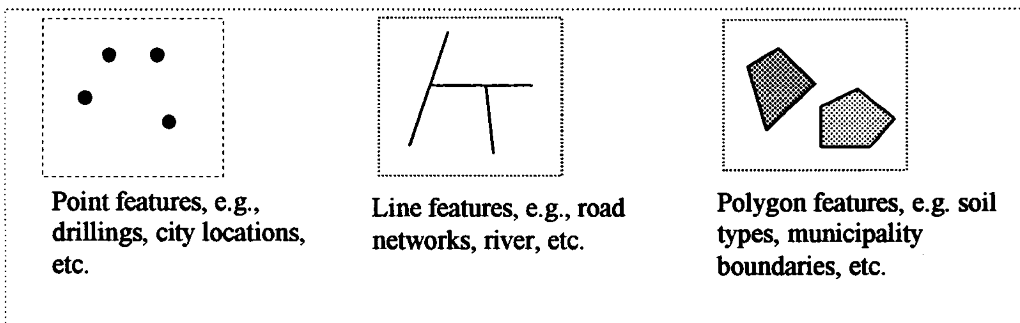


**Figure 3-5:** Three types of vector data in a GIS environment.

#### 3. 3. 1. 1 Geometric calculation

Previous karst investigators have developed and used numerous measurements to illustrate the morphometric characteristics of karst landforms. In this study, a list of major morphometric measurements were applied to the geospatial data of the study area using vector operational functionalities in a GIS environment. The development and distribution of sinkholes have been often used to indicate karstic evolution according to the geometric measurements (Table 3-3 and Figure 3-6). Any individual sinkhole can be defined and expressed by various ratios between lengths and widths, and its internal shape with respect to the drainage focus can be assessed with the product of symmetry and aspect ratio (Williams, 1972b).

When performing geometric measurements of sinkholes it is important to determine the spatial locations of sinkholes. Williams (1972b) suggested the use of a swallet, i.e. the lowest point where water disappears underground, to represent the spatial location of a sinkhole. Yet, it was challenging to locate swallets because of dense vegetation or thick covering soil layers. An alternative solution was to use the centroids of the sinkhole polygons (e.g., their topographic boundaries) to represent their locations. The centroids of the sinkhole polygons were extracted using a built-in function of ArcGIS (Shapes to centroids) based on the geometric shapes of the polygons, and were stored as point features.

**Table 3-3:** Geometric measurement of sinkholes.

| Parameters | Definition |
|---|---|
| Length: $L$ | The length of the long axis |
| Width: $W_{max}$ | The longest distance across, perpendicular to long axis |
| Area: $A_{si}$ | Measured based on a contour drawn at the break in slope at the edge of the sinkhole |
| Length ratio: $R_L = L_1 / L_2$ | ($L_1$ and $L_2$: longest and shortest parts respectively of the sinkhole long axis on either side of the lowest point) |
| Width ratio: $R_W = W_1 / W_2$ | ($W_1$ and $W_2$: longest and shortest parts respectively of the sinkhole width axis on either side of the lowest point, measured at right angles to the length axis) |
| Product of symmetry: $P_s$ | $R_L \cdot R_W$ the product of length and width ratios |
| Aspect ratio (Eccentricity): $R_{LW} = (L_1 + L_2) / W_{max}$ | A value that defines the shape of an ellipse |

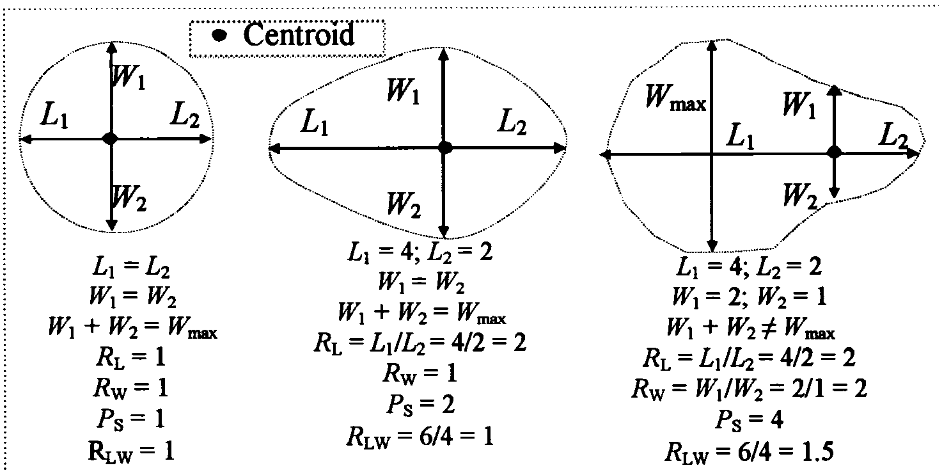


**Figure 3-6:** An illustration of plane geometry of sinkholes (Williams, 1972b).

In addition to geometric measurements of sinkholes, four measures: the sinkhole density $D_s$, the mean sinkhole area $\overline{A}$, the sinkhole area ratio $R_s$, and the pitting index $R_p$ have been devised (Williams, 1969) to describe the spatial development of sinkholes (Table 3-4). The sinkhole density was obtained by counting all the sinkholes within the karstic lands under study and dividing by the land area. The sinkhole density represents the number of entry points of internal runoff water into the subsurface, while the mean sinkhole area represents the development of sinkholes in terms of their dimensions. The sinkhole area ratio was determined as the sum of individual sinkhole areas divided by the total area of karst lands. The pitting index was used to indicate the degree of karstification of the karstic land.

**Table 3-4:** Measurements of spatial development (Williams, 1969).

| Parameters | Definition | |
|---|---|---|
| $D_s$: Sinkhole density | $N_s/A_K$ | $N_s$ = Numbers of the sinkholes in the karstic lands |
| $\overline{A}$: Mean sinkhole area | $\sum_i A_{si} / N_s$ | $A_k$ = Area of karstic lands |
| $R_s$: Sinkhole area ratio | $\sum_i A_{si} / A_K$ | $\sum_i A_{si}$ = Total sinkhole areas |
| $R_p$: Pitting index | $A_K / \sum_i A_{si}$ | |

### 3. 3. 1. 2 Distribution pattern of points – nearest neighbour analysis

The nearest neighbour analysis developed by Clark and Evans (1954) was applied to investigate sinkhole distribution patterns. This analysis assesses patterns with a nearest neighbour index $\overline{R}$ (Eq. 3.2) that compares the mean actual distance $\overline{L_a}$ between points in a spatial distribution with the mean expected distance $\overline{L_e}$ (Eq. 3.1) (e.g., points are randomly arrayed). Sinkhole distribution patterns and their corresponding nearest neighbour index can be classified as regular, random or clustered (Figure 3-7 ) based on the value of $\overline{R}$, which varies from 0 for an array with maximum aggregation or clustering, through 1 for a random layout, to 2.149 and above for a regular pattern (Table 3-5).

$$\overline{L_e} = \frac{1}{2\sqrt{D_s}} \quad ; D_s\text{: sinkhole density (see Table 3.4).} \qquad (3.1)$$

$$\overline{R} = \frac{\overline{L_a}}{\overline{L_e}} \qquad (3.2)$$

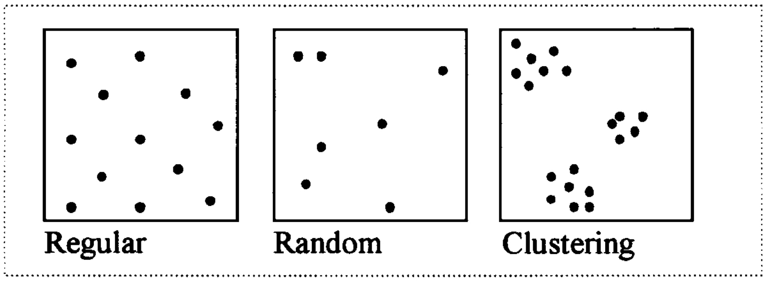


**Figure 3-7:** Illustrations of sinkhole dispersion patterns.

**Table 3-5:** Sinkhole distribution patterns and their corresponding nearest neighbour index (Ford and Williams, 1989).

| Sinkhole distribution patterns | Nearest neighbour index $\overline{R}$ |
|---|---|
| Clustering | $0 \leq \overline{R} < 1$ |
| Random | $1 \leq \overline{R} < 2.149$ |
| Regular | $2.149 \leq \overline{R}$ |

Given that conventional map-based measuring methods for determining the nearest neighbour of individual sinkholes and the distances between them are time consuming and demanding, calculating $\overline{L_a}$ can be difficult. To facilitate this task, a public domain Visual Basic application developed by Sawada (2002) was implemented as an additional ArcGIS toolbar selection in this study. A nearest neighbour distance and an identification of the nearest neighbour for individual points were obtained using this application. The mean actual distance $\overline{L_a}$ of a sinkhole field or karst area was then calculated by averaging the nearest neighbour distances of the sinkholes in the investigated karst area. Sawada's nearest neighbour analysis application provides a mean modified nearest neighbour index $\overline{R_c}$ and a mean modified expected distance $\overline{L_{ec}}$ ( Eq. 3.3, 3.4).

$$\overline{L_{ec}} = \frac{1}{2}\sqrt{D_s} + \frac{P}{N_s}\left(0.0514 + \frac{0.041}{\sqrt{N_s}}\right) \qquad (3.3)$$

$$\overline{R_c} = \frac{\overline{L_a}}{\overline{L_{ec}}} \qquad (3.4)$$

$D_s$: sinkhole density ($km^{-2}$)

$P$: perimeter of a karst area (km)

$N_s$: number of sinkholes

According to Sawada (2002), the modified nearest neighbour index was developed for several reasons. Because the mean is not a robust indicator and reflexive neighbours are often high. Meanwhile, the nearest neighbour index $\overline{R}$ of Clark and Evans (1954), based on the mean nearest neighbour distance between all points, is not very useful for hypothesis testing of point-patterns. The modified nearest neighbour index $\overline{R_c}$

is a function of the area and perimeter of the study region, taking into account the influence of region size and shape. In this study, the modified and non-modified nearest neighbour indexes were both examined.

### 3. 3. 1. 3 The nearest features – distance between points and lines

A spatial joining of points and lines layers was used to investigate spatial correlation between the development of sinkholes and dry gullies. With a spatial join, each point (i.e., a sinkhole centroid) was assigned all the attributes and the distance of the line (e.g., a gully segment) closest to it (Figure 3-8). Having examined the relationship between sinkholes and gully development, Day (1983) suggested that the two features compete such that whichever is favored by contemporary hydrologic conditions develops at the expense of the other. He also stated that: "Distance to nearest gullies is a measure similar to the estimated mean probability flow distance, and it indicates the relative location of the quadrate within a theoretical groundwater flow system."

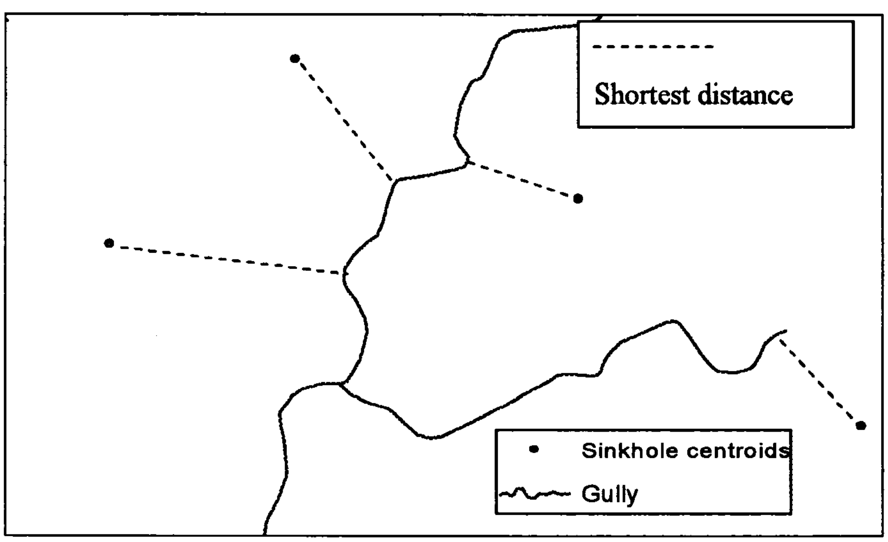


**Figure 3-8:** Shortest distances between gullies and sinkholes.

### 3. 3. 1. 4 Orientation of lines

The investigation of the orientation of line features (also called lineament), i.e., sinkhole long axis, and sinkhole alignments, was conducted using Lineament analysis (Gyoobum, 2004) and Rose diagrams (Chen, 2005) in ArcGIS. The lineament analysis tool was used to remove duplicated tiny lineaments from input errors in the digitizing process, and also used to generalize curved lineaments. After optimizing line features, the lineament orientation can be calculated. Meanwhile, a Rose diagram tool was used to display statistics of directional data (Figure 3-9). The circumference of the circle was split into groups (or bins) based on the direction (i.e., 0° ~ 180°) of the lines. The radii of the groups were the relative frequencies of the summed lengths of the lines of each group (Williams, 1972b). Additionally, a number of lineament properties of the input lines: node to node, line best fit, line segments, etc. (see Figure 3-10) could be analyzed using the rose diagram.

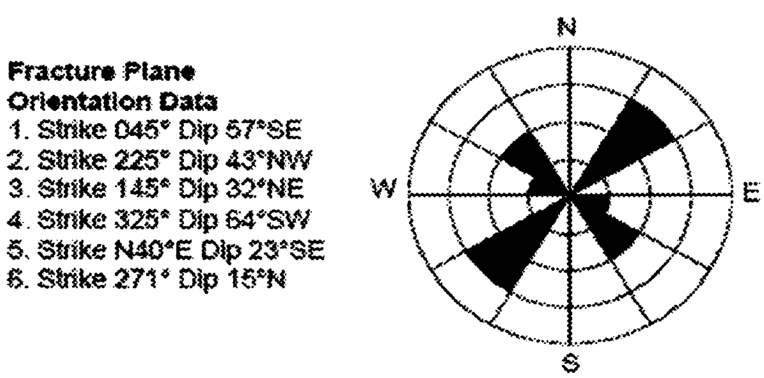


**Figure 3-9:** An example of a Rose Diagram.

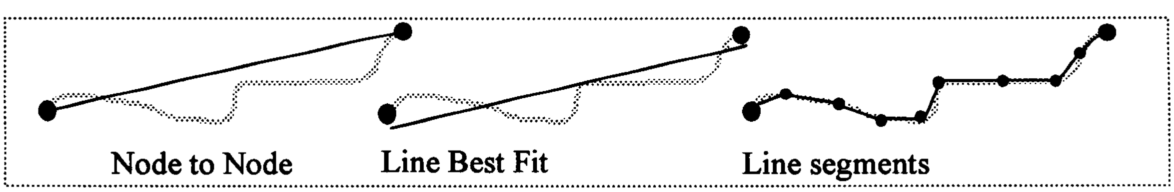


**Figure 3-10:** Directional types of line features.

### 3. 3. 2 Raster operations – surface interpolation

ArcGIS's raster functionality was used in the study to create DEMs of the study area. Those DEMs were stored in raster (or grid) format, a spatial data model defining space as an array of equally sized cells containing attribute values and location coordinates. The creation of DEMs was based on the tool TOPOGRID, a surface interpolation method based on the application ANUDEM developed by Hutchinson (1989). This surface interpolation method was used because of its capability of adding various surface elevation sources from contours, streams, points, sinks, or boundaries, to enhance the representation of a drainage system in a DEM. The creation of DEMs, within the context of the study served to obtain continuous elevation models for the surface and subsurface of the study area. The surface DEM was derived from the digitized contours obtained from 1:2,500 scale topography maps, and from bathymetric data for the coastal regions of the study area. The subsurface DEM was derived from the 1:10,000 scale digitized contours presenting the elevations of the coral base.

The determination of the DEM's accuracy was based on the horizontal and vertical resolution of DEMs. The latter by comparing the DEM-generated elevations with "true" values of elevation measured in the field, which were from the spot heights marked on the hardcopy source. The former by the size of the pixel. Comparison statistics included the root mean square error (RMSE; Eq. 3.5) and the mean error (ME; Eq. 3.6) (Wise, 1998). According to Wise (1998), an RMSE of half a contour interval or less is required to allow a good quality of terrain analysis. The ME is used to measure whether the DEM is systematically under- or over-estimating elevation:

$$RMSE = \sqrt{\frac{\sum_{i=1}^{n} d_i^2}{n}} \tag{3.5}$$

Where $d_i = Z_{\text{int}} - Z_{true}$

$Z_{\text{int}}$: Interpolated DEM elevation of a test point

$Z_{\text{true}}$: True elevation of a test point

$n$: number of test points

$$ME = \frac{\sum_{i=1}^{n} d_i}{n} \tag{3.6}$$

# CHAPTER 4 RESULTS AND DISCUSSIONS

## 4. 1 Digital elevation models

The surface DEM (Figure 4-1) was derived from combining the contours of thirteen 1:2,500 scale topographic quadrangles (interval: $\approx$ 3.3 m) and sounding depths from bathymetric data. It was stored in ESRI GRID format at a cell-size of $5\times5$ m$^2$. The root mean square error (RMSE; Eq. 3.5) and the mean error (ME; Eq. 3.6) were used to compare marked spot heights on the 1:2,500 scale set of topographic quadrangles, taken as true ground elevations, to elevations on the DEM at each of 85 check-points (Figure 4-1). At 0.015 m, the surface DEM's RMSE with respect to vertical accuracy (Table 4-1) met the required RMSE criterion (RMSE < 1.50 m) according to section 3.3.2. The ME showed the elevation of the surface DEM to be over-estimated by 0.035 m.

The sub-surface DEM (Figure 4-2) was derived from coral base elevations given in 1:10,000 scale geology quadrangles and stored in the same format as the surface DEM. However, since the elevations of the coral base did not vary sharply, the cell-size was set at 10m $\times$10m. This had the added benefit of increasing computer processing speed when conducting further analyses. Coral base elevations presented in the upper right-hand corner of the sub-surface DEM (elevation > 300 m) were roughly interpolated given the absence of coral/rock elevations for the Scotland District. Values of RMSE and ME for the sub-surface DME (Table 4-1) were based on a comparison to 42 check-points (Figure 4-2) drawn from well drilling logs. While elevations of the sub-surface DEM were overestimated by 0.28 m, the RMSE for vertical accuracy of 1.63 m was below the RMSE criterion (according to the section 3.3.2) of 5 m.

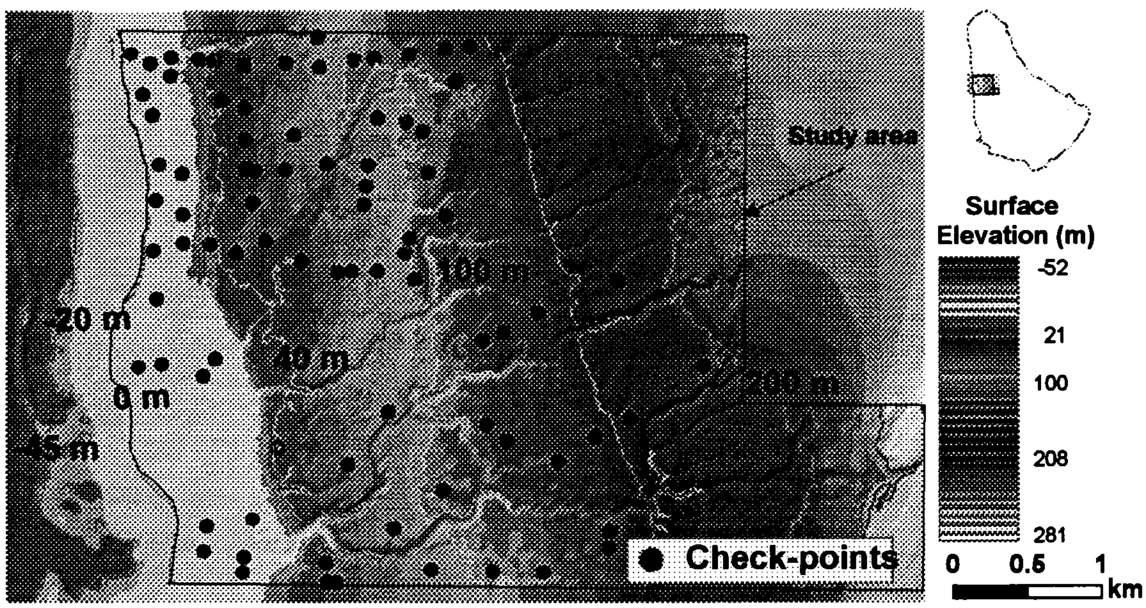


**Figure 4-1:** The surface DEM, produced from 1:2,500 scale topographic quadrangles, covering the studied karst area, and the locations of the 85 check-points used for the quality assessment of this DEM.

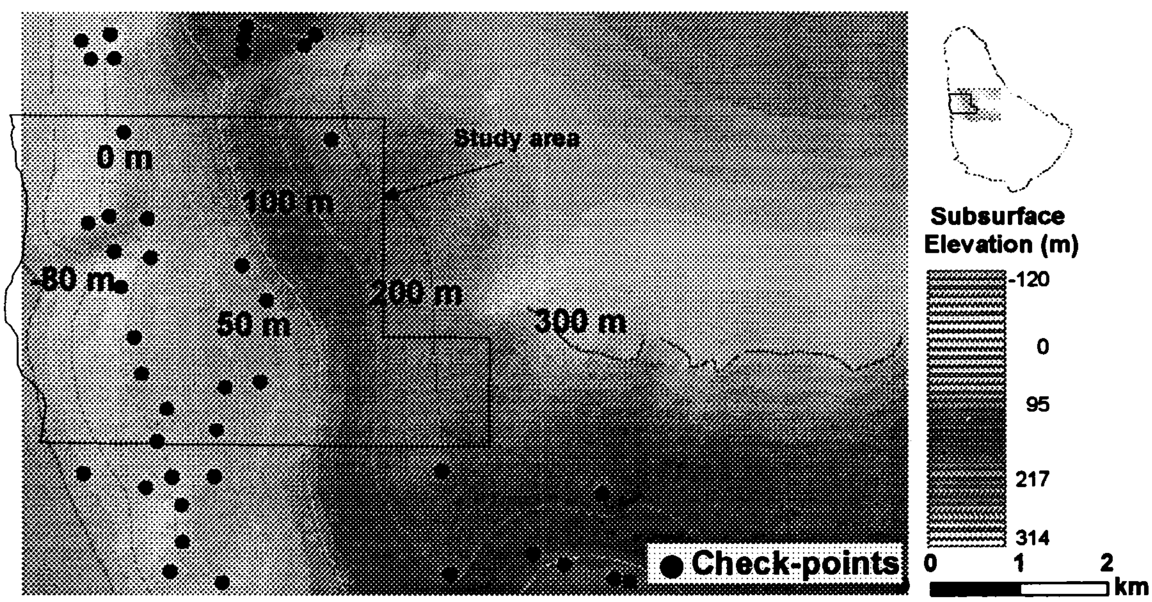


**Figure 4-2:** The subsurface DEM, produced from 1:10,000 scale geology quadrangles, representing the coral base elevation beneath the studied karst area, and the locations of the 42 check-points used for the quality assessment of this DEM.

**Table 4-1:** The quality assessment of the surface DEM and the subsurface DEM using root mean square error (RMSE) and mean error (ME) based on a comparison to their check-points (Unit: m).

| DEM | Min. error | Max. error | ME | RMSE | Required RMSE |
|---|---|---|---|---|---|
| Surface | -0.49 | 0.6 | 0.035 | 0.15 | <1.5 |
| Sub-surface | -2.86 | 3.53 | 0.28 | 1.63 | <5 |

### 4. 1. 1 The thickness of coral rock beneath the karst area under study

A raster file (ArcGIS GRID) showing the thickness of coral cap beneath the study area surface was interpolated from a 10 m grid of surface to sub-surface elevation differences (Figure 4-3). No data were available at the western edge of this raster (≈ 0.007 km$^2$) as the sub-surface DEM map did not extend as far west as the surface DEM map. As presented in Figure 4-3, the thickness of coral rock beneath the surface of the studied karst area, ranging from 0 to about 110 m, increased towards the sea. The thickness of the coral rock was measured at each sinkhole location within the studied karst area. As discussed below these data were used to assess whether certain thickness of the bedding coral rock favoured the development or altered the distribution of sinkholes.

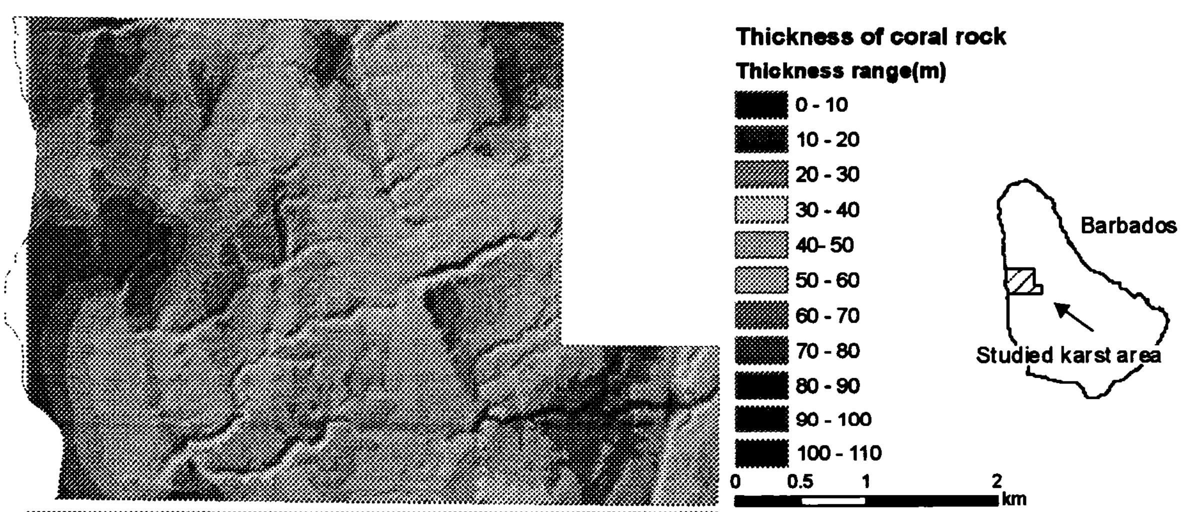


**Figure 4-3:** The thickness of coral rock beneath the surface of the studied karst area.

### 4. 2 Characteristics of sinkhole geometry

### 4. 2. 1 Shape and size

Within the 16.41 km$^2$ karst area under examination (Figure 4-4), the shapes and sizes of 76 sinkholes were investigated using five geometric parameters: sinkhole area ($A_{si}$; Figure 4-5a), length ratio ($R_L$), width ratio ($R_W$), product of symmetry ($P_S$; Figure 4-5b), and aspect ratio ($R_{LW}$; Figure 4-5c). The area of sinkholes varied from 44.83 to 10918.38 m$^2$ and roughly 90% were of < 5,000 m$^2$ (Figure 4-5a). The product of symmetry varied slightly, ranging between 1 and 2, indicating that the sinkholes tend to form in symmetric shapes (Figure 4-5b). Over 90 % of aspect ratios were between 0.99 and 2.0 suggesting that the sinkholes are generally near ellipsoid in plan view.

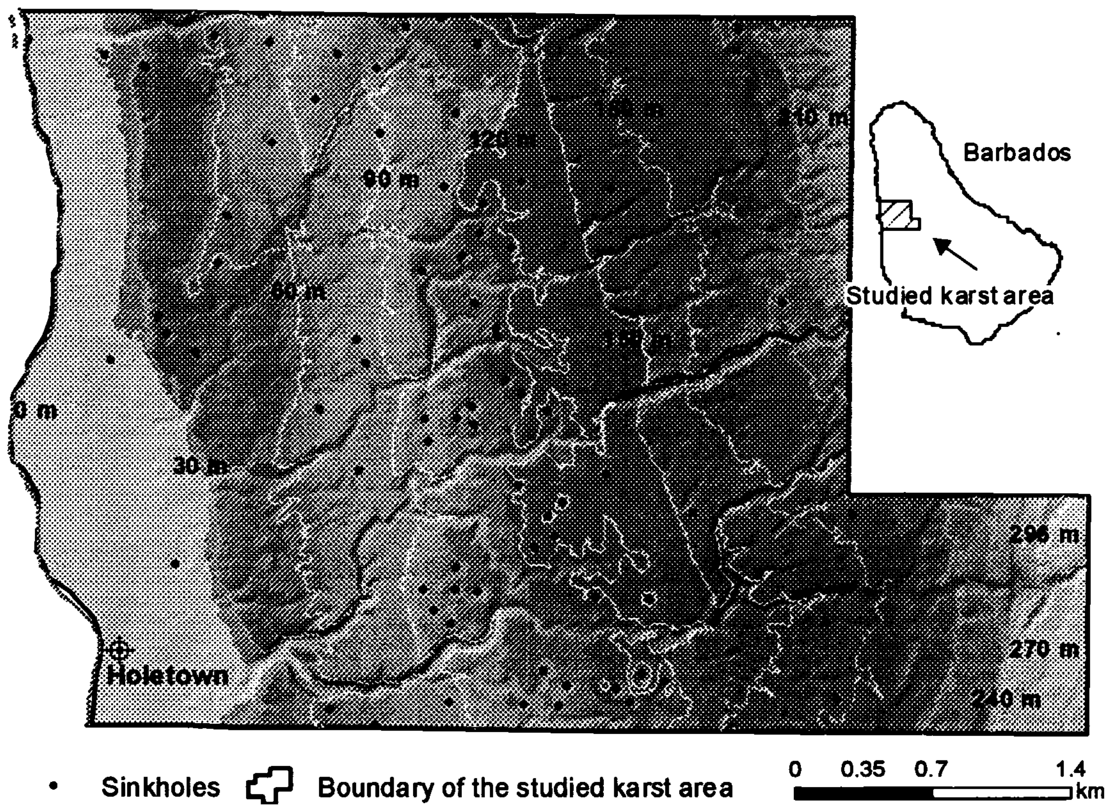


**Figure 4-4:** Location of 76 sinkholes present in the karst area under study.

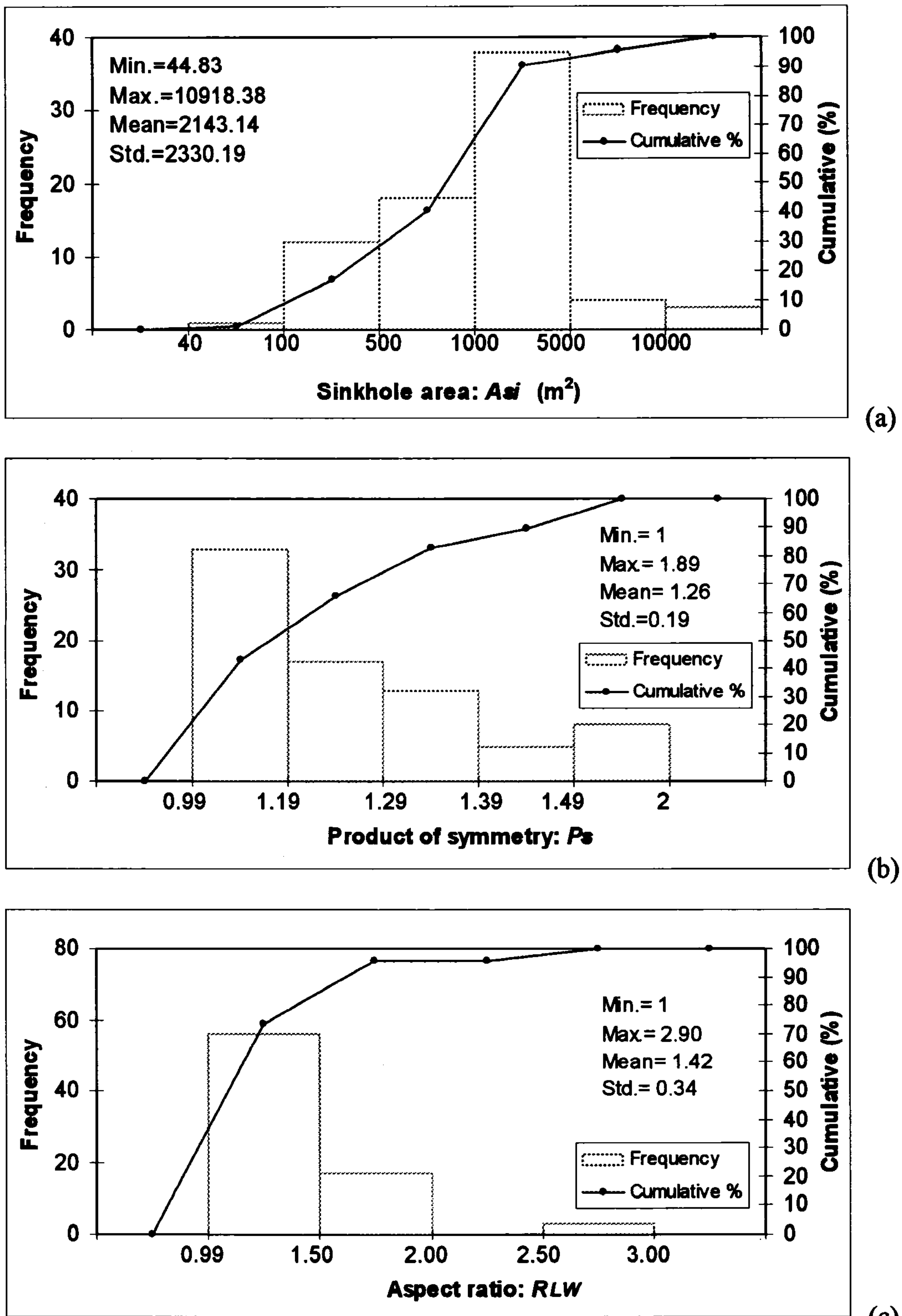


**Figure 4-5:** Frequency distribution of sinkhole geometric parameters for 76 sinkholes present in the karst area under study. (a) sinkhole area, (b) product of symmetry, (c) aspect ratio.

The shapes of the sinkholes tend to be elliptical, a power function ($L = 0.83 \cdot W_{max}^{0.97}$, $R^2 = 0.87$) was found which describes a strong relationship between the length ($L$) and width ($W_{max}$) of the sinkholes investigated (Figure 4-6). This indicates that the sinkholes tend to become more elongated as they grow larger. This kind of allometric growth has been noted in other karstic studies (Kemmerly, 1976; Kemmerly and Towe, 1978; Brook and Allison, 1986; Gutiérrez-Santolalla *et al.*, 2005). Yet, since the exponent of this power function (Figure 4-6) is close to unity, allometric growth is not a marked tendency; coinciding with the findings of [1]Day (1983) in northern Barbados.

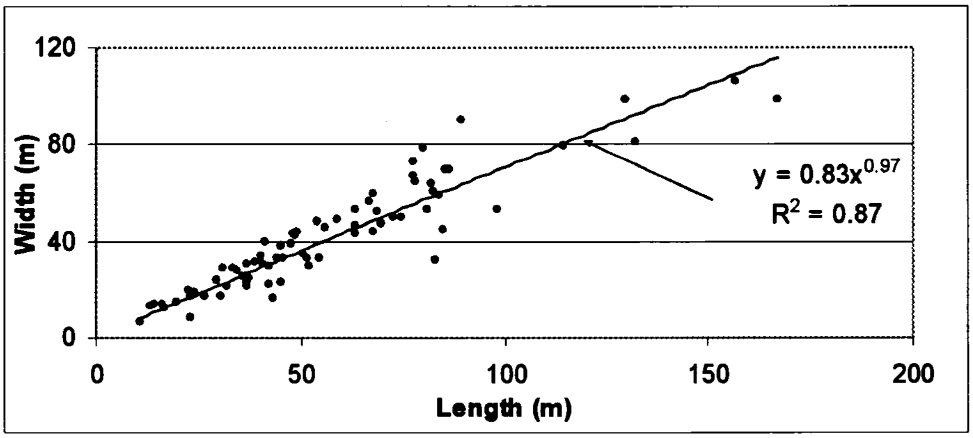


**Figure 4-6:** Relationship of sinkhole length and width for 76 sinkholes present in the karst area under study.

To assess whether significant sinkhole allometric growth occurs at different elevation ranges, the aspect ratio $R_{LW}$, was compared at different elevation ranges (Table 4-2 and Figure 4-7). The elevation of each sinkhole was interpolated from the constructed surface DEM according to the location of the sinkhole centroid. The mean length of the major axis, maximum width, and reciprocal of the aspect ratio were obtained for eight 30-m interval elevation classes (Table 4-2). No correlation is apparent in either this study or

[1] The author was not able to isolate the data of Day (1983) specific to this study area. Day's work entailed all of northern Barbados; therefore, a direct comparison was not possible.

that of Day (1983) on the island of Barbados. Thus sinkhole allometric growth and any correlation with elevation is likely site specific. Yet, significant sinkhole allometric growth has been found in other karst investigations; for example, Florida sinkholes were found to present a greater circularity with increasing elevations (Denizman and Randazzo, 2000).

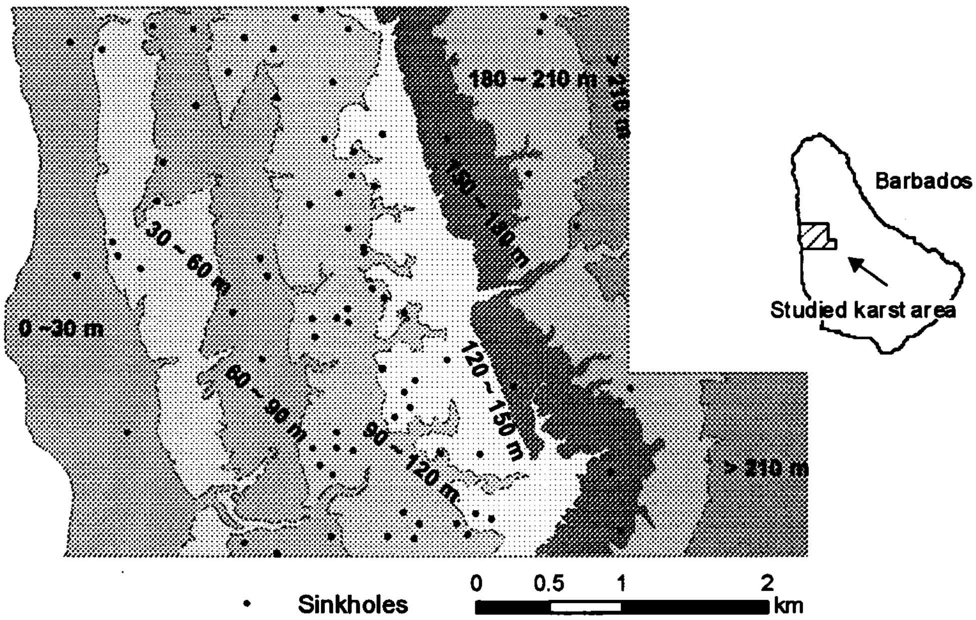


**Figure 4-7:** Sinkholes grouped into eight elevation ranges.

**Table 4-2:** Mean sinkhole geometry parameters in different elevation ranges.

| | This study | | | | Day (1983) | | |
|---|---|---|---|---|---|---|---|
| Location | Porters & Trends groundwater catchments (≈16.41 km$^2$) | | | | Northern Barbados (≈124.40 km$^2$) | | |
| Elevation (m) | $\overline{A}$ (m$^2$) | $\overline{L}$ (m) | $\overline{W_{max}}$ (m) | $1/\overline{R_{LW}}$ | $\overline{L}$ (m) | $\overline{W_{max}}$ (m) | $1/\overline{R_{LW}}$ |
| 0-30 | 1564.33 | 51.31 | 37.78 | 0.77 | 26.46 | 17.44 | 0.69 |
| 30-60 | 1159.08 | 38.74 | 32.57 | 0.81 | 43.48 | 31.02 | 0.72 |
| 60-90 | 1821.31 | 54.46 | 33.70 | 0.64 | 34.74 | 26.36 | 0.73 |
| 90-120 | 2321.61 | 58.66 | 43.94 | 0.76 | 40.18 | 30.98 | 0.78 |
| 120-150 | 2910.44 | 62.68 | 48.08 | 0.76 | 57.80 | 43.44 | 0.58 |
| 150-180 | 1039.88 | 37.84 | 26.23 | 0.63 | 43.44 | 35.88 | 0.80 |
| 180-210 | 2433.30 | 62.68 | 48.02 | 0.80 | 50.72 | 39.72 | 0.62 |
| 210-240 | 2815.43 | 39.94 | 44.96 | 0.53 | 66.40 | 50.52 | 0.77 |

$\overline{A}$ : mean sinkhole area; $\overline{L}$ : mean long axis length; $\overline{W_{max}}$ : mean maximum width; $1/\overline{R_{LW}}$ : reciprocal of mean aspect ratio.

### 4. 2. 2 Sinkhole long-axis orientation

Rose diagrams were used to present statistics on the orientation and magnitude of individual sinkhole long axes (Figure 4-8a; 76 sinkholes). The results show that there is no specific sinkhole long-axis orientation in the study area because any one orientation is not uniquely statistically-significant (Chi-square). However, visually a northeast trend is apparent (Figure 4-8a). Also with the NE orientation there are two major grouping, 60°-70° (15.83 % of total long-axis length) and 20°-30° (13.59 % of total long-axis length). According to Figure 4-9, the spatial distribution of these sinkholes, those falling into the two common orientations, does not seem to be controlled by any particular hydrogeologic settings. As shown in Figure 4-9, most of these sinkholes do occur at elevations between 90 m to 120 m. However, these sinkholes are randomly distributed in this elevation range. Further, there are 24 other sinkholes that have different azimuth orientations also distributed in the same region.

Similar trends in sinkhole orientation (northeast) (Figure 4-8b) were also found for northern Barbados by Day (1983). The most common orientation class (10°-20°; 11.61 % of total long-axis length) in his analysis was also not significantly different so as to claim a specific sinkhole orientation for northern Barbados. To be noted, the study area (124.4 $km^2$) and the number of investigated sinkholes (1179 sinkholes) of Day (1983) are much larger than those of author's (16.41 $km^2$, 76 sinkholes). The one can conclude (more based upon Day's 1179 sinkholes) that though there is a trend to a NE long-axis orientation, there remains no statistically and significantly unique orientation.

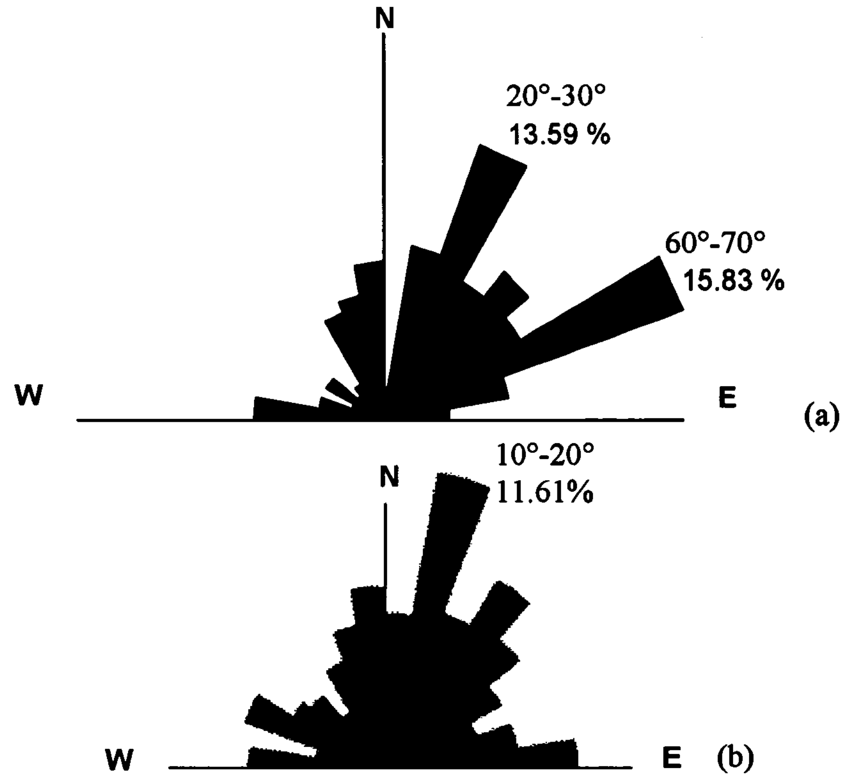


**Figure 4-8:** Rose diagram showing sinkhole long-axis orientation in (a) the study area, and (b) in Day's (1983) study of northern Barbados

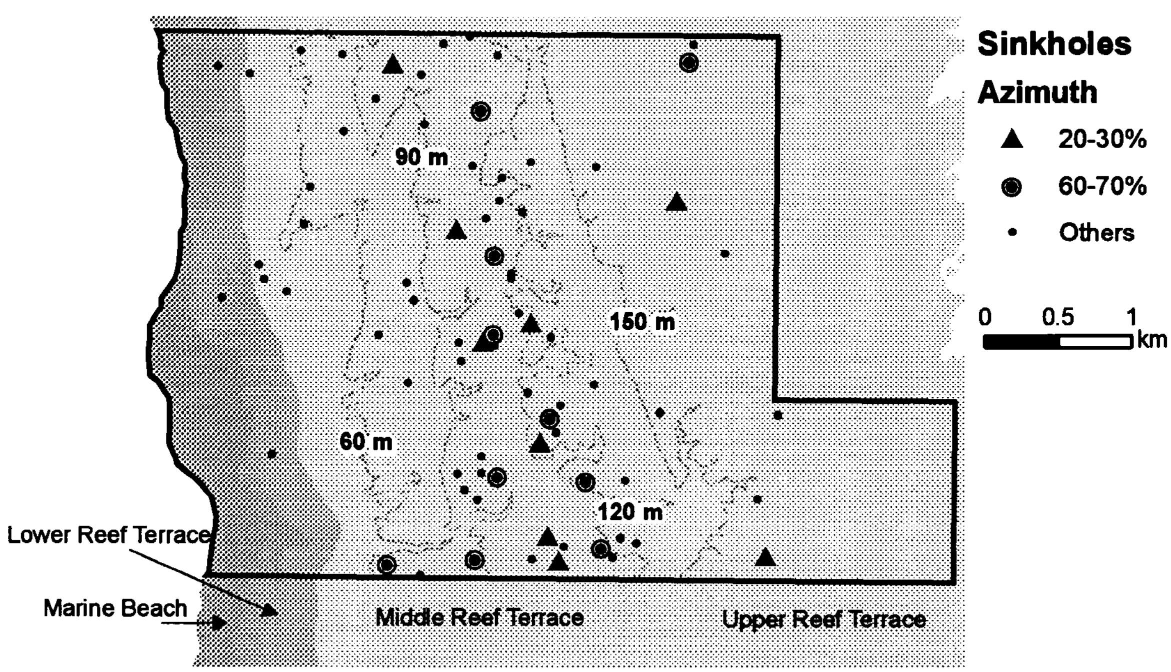


**Figure 4-9:** Spatial distribution of the sinkholes falling in 20-30 % and 60-70 % orientation (azimuth) groups.

## 4. 3 Spatial development and distribution of sinkholes in a karst area

### 4. 3. 1 Density and pitting index

The spatial development of sinkholes in the karst area under study was investigated using sinkhole density ($D_s$), mean sinkhole area ($\overline{A}$), area ratio ($R_s$), and pitting index ($R_p$) (Table 4-3). Sinkhole density is 4.63 km$^{-2}$ for the 76 sinkholes in the 16.41 km$^2$ area investigated. The total area occupied by the 76 sinkholes is approximately 0.16 km$^2$, representing almost 1% of the total area under study, resulting in an area ratio and pitting index of 0.01 and 100.75, respectively. Although Day (1983) claimed an under-estimation of sinkhole numbers due to difficulties of identifying small sinkholes from aerial photography, his sinkhole density is roughly twice that in this study. Therefore, it would mean that the author's study area is an area, for Barbados, with an exceptionally low sinkhole density. Comparing the sinkhole density measured in this study to those of other tropical karst regions (Table 4-4), the development of sinkholes on the island of Barbados is similar to that in the Yucatan (Day, 1978). The level of karstification (i.e., pitting index) in the study area is similar to that obtained by Day (1983) in northern Barbados. This suggests a consistent karstification pitting across the northern parts of the island of Barbados.

**Table 4-3:** Sinkhole development parameters for Barbados karst

| Sinkhole development parameters | This study<br>Porters & Trends groundwater catchments (≈16.41 km$^2$) | Day (1983)<br>Northern Barbados (≈124.4 km$^2$) |
|---|---|---|
| $D_s$ (km$^{-2}$): sinkhole density | 4.63 | 9.47 |
| $\overline{A}$ (m$^2$): sinkhole mean area | 2143.14 | 1223.00 |
| $R_s$ : area ratio | 0.01 | 0.011 |
| $R_p$ : pitting index | 100.75 | 90.91 |

**Table 4-4:** Sinkhole densities of other tropical karst regions.

| Karst region | Sinkhole density ($km^{-2}$) | Sources |
|---|---|---|
| New Guinea | 13.05~13.50<br>10.50~22.10 | Williams (1971)<br>Williams (1972a) |
| Antigua | 0.39 | Day (1978) |
| Yucatan | 3.34 | Day (1978) |
| N. Jamaica | 2.85 | Day (1978) |
| Guatemala | 13.10 | Day (1978) |
| Belize | 9.70 | Day (1978) |
| Guadeloupe | 11.20 | Day (1978) |

There are different investigations on sinkhole density based on topographic maps or aerial photography in different areas of Barbados. Table 4-5 presents sinkholes density in different elevation classes (30-m ranges) conducted by Fermor (1972), Day (1983), and Wandelt (2000) (Table 4-5). The four datasets all appear a weak correlation between elevation and sinkhole density, and their highest sinkhole densities similarly occur at 90-120 m elevation range (120-149 m for Day's results).

The most comparable results are those of Wandelt (2000) based on 1:10,000 aerial photography. Sinkhole densities of Wandelt's study were calculated by author based on Wandelt's sinkhole maps. For the same area, Wandelt (2000) and author's results show similar values on sinkhole density and similar trends with elevation. However, significant differences appear between Day's (1983) and Fermor's (1972) studies, likely attributable to differences in methodology and area studied. Fermor (1972) stated that his sinkhole density was likely an underestimate given that small sinkholes were not likely to appear on the 1:10,000 topographic maps (6-m contour-interval) he used. Although Day (1983) obtained a greater sinkhole density in northern Barbados, further investigations in the same region are needed to determine whether more sinkholes develop in that region or false sinkholes were included in the data used by Day.

**Table 4-5:** Sinkhole density versus elevation ranges of Barbados karst

| | This study (2004) | Wandelt(2000) | Day (1983) | Fermor (1972) |
|---|---|---|---|---|
| Data Source | Topographic map, 3.3-m interval (1977) | 1:10,000Aerial photography (2000) | 1:10,000Aerial photography 1964 | Topographic map, 6-m interval (older than 1972) |
| Study Area | Porters and Trends groundwater catchments (≈ 16.41 $km^2$) | | Northern Barbados (≈ 124.4 $km^2$) | Whole island (≈ 432.20 $km^2$) |
| Elevation(m) | Sinkholes density ($km^{-2}$) | | | |
| 0-30 | 1.20 | 2.79 | 3.46 | 1.6 |
| 30-60 | 3.05 | 3.66 | 9.42 | 4.4 |
| 60-90 | 5.65 | 5.66 | 10.18 | 6.8 |
| 90-120 | 13.71 | 11.23 | 13.66 | 9.4 |
| 120-150 | 4.02 | 5.02 | 13.86 | 7.3 |
| 150-180 | 2.33 | 1.73 | 11.05 | 8.7 |
| 180-210 | 1.87 | 1.87 | 8.16 | 6.8 |
| 210-240 | 1.03 | 2.06 | 6.11 | 4.3 |

Furthermore, sinkhole density and pitting have been often used to determine the degree of karstification in a karst area. Coleman and Balchin (1959), using a karstification model developed in Barbados, determined that the age of the surface can be roughly estimated by equating each metre in elevation to approximately 3000 years of emergence. Applying this model, larger sinkholes investigated in this study appear in the area with age about 450,000 years old (i.e., surface elevation 150 m) (Table 4-2).

A similar tendency is found for sinkhole density (Table 4-5). Further, as shown in Table 4-5, the 100-m contour range is the range in which the largest sinkhole density and pitting occur. This greater sinkhole development which occurs at the 100-m elevation range is likely to be the consequence of the greater infiltration capacity, as found by Fermor (1972) of the Coral Cap less than 300 000 years old. This is also supported by recent hydrogeologic studies conducted by Jones *et al.* (2000) and Jones (2002 and 2003) using oxygen isotopes; that at the 100-m contour range a large amount of discrete recharge to the aquifer (> 250 mm $h^{-1}$) occurs.

Although the geologic and physiographic environment at different altitude ranges may be similar, the distribution of the sinkholes in the study area shows significant patterns suggesting a favoured trend of sinkhole spatial occurrence within the middle terrace (30 – 150 m elevation). That is, the Middle terrace coincides with the 100-m contour range (300,000 year BP). As shown in Figure 4-10 three separate coral reef terraces are evident. It is also evident that most karstification occurs on the middle terrace based on the highest sinkhole density and lowest pitting index; 7.59 $km^{-2}$ and 59.56 respectively. Even though the Upper terrace is older (exposed to karstification longer), it is less karstified. The fact that the middle terrace is more karstified leads one to conclude that its material makeup is likely more fractured, encouraging infiltration/dissolution (see section 1.2). Further, the chemical makeup of the middle terrace could be such that it is more susceptible to dissolution. Denizman and Randazzo (2000) based on a study in the lower Suwannee river basin, Florida, also found that degree of karstification of any one terrace was not related to age of that terrace; some younger terraces were more highly karstified than older ones.

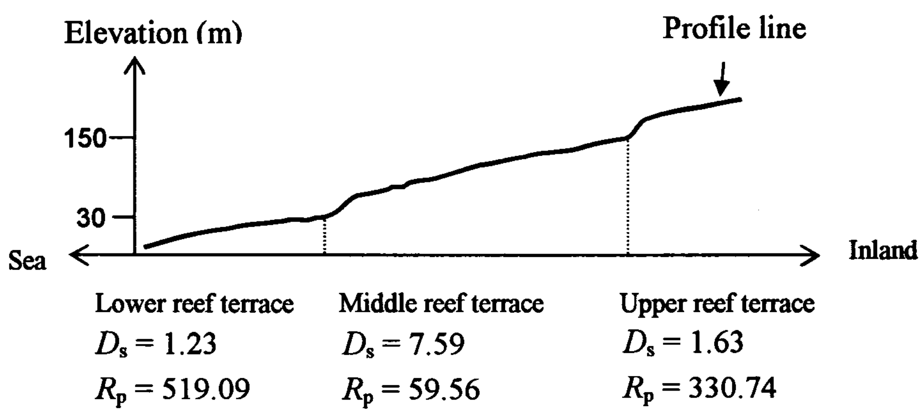


*$D_s$: sinkhole density ($km^{-2}$); $R_p$: pitting index

**Figure 4-10:** Cross-section profile of the coral reef terraces in the area under study with the sinkhole density and pitting index of each.

On the other hand if one examines sinkhole average area (per sinkhole; Table 4-2) and sinkhole density (Table 4-5), it is evident that degree of karstification is age related within the middle terrace. There are not enough sinkholes in the lower or upper terrace on which to make a similar conclusion.

### 4. 3. 2 Sinkhole clusters

Sinkholes were treated as points defined at their centroids. Clark & Evans' (1954) nearest neighbour index $\overline{R}$ (Eq. 3.2) and Sawada's (2002) modified nearest neighbour index $\overline{R}_c$ (Eq. 3.4) were calculated to investigate the distribution pattern of sinkholes. Sawada (2002) made an effort to improve on the approach of Clark and Evans (1954) by incorporating size and shape of the study area. One of the required parameters $L_a$, the actual distance of neighbouring sinkholes, was obtained using Sawada's GIS application. The frequency distribution of $L_a$ (Figure 4-11) shows that distance between two sinkhole neighbours in the study area ranges from 0.04 km to 1.04 km, and that about 80% of the sinkholes are less than 0.3 km from their nearest neighbour.

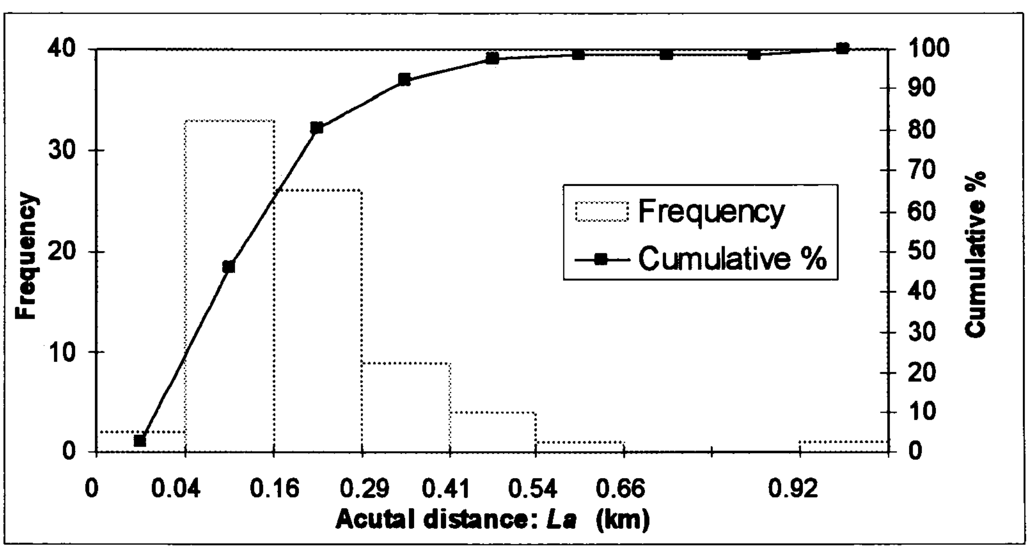


**Figure 4-11:** Frequency distribution of actual distance between neighbouring sinkholes.

The values of $\overline{R}$ and $\overline{R_c}$ were obtained and shown to be both below 1.0 (Table 4-6). This suggests that sinkholes in the karst area under study tend to form clusters (Figure 4-12). The value of $\overline{R}$ (0.93) is greater than $\overline{R_c}$ (0.20) because the mean modified expected distance $\overline{L_{ec}}$ = 1.09 km (Eq. 3.3) is 3.7-fold greater than the mean expected distance $\overline{L_e}$ = 0.23 km (Eq. 3.1); $\overline{L_{ec}}$ being affected by size and shape of study area. This shows that by taking into account size and shape, at least for this study, definition of clustering is more evident. Furthermore, based on visual interpretation the sinkhole clusters (Figure 4-12) tend to be elongated. The principal sinkhole cluster elongation direction of northeast is similar to that of the long-axis of sinkholes themselves.

**Table 4-6:** The results of sinkhole distribution pattern in the karst area.

| | Clark and Evans (1954) Nearest neighbour index | | | | Sawada (2002) Modified nearest neighbour index | | | |
|---|---|---|---|---|---|---|---|---|
| Parameters | $\overline{L_a}$ (km) | $\overline{L_e}$ (km) | $\overline{R}$ | Pattern | $\overline{L_a}$ (km) | $\overline{L_{ec}}$ (km) | $\overline{R_c}$ | Pattern |
| Result | 0.22 | 0.23 | 0.93 | Clustering | 0.22 | 1.09 | 0.20 | Clustering |

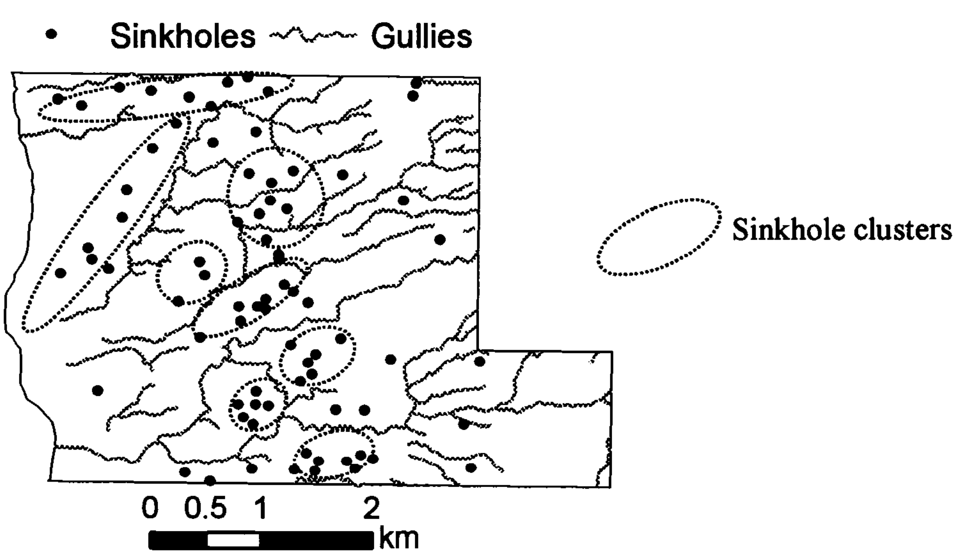


**Figure 4-12:** Illustrating sinkhole clusters and gullies.

Furthermore, the same sinkhole cluster pattern was similarly investigated within each elevation range using both Clerk & Evans'(1954) and Sawada's (2002) indices and was compared with the analysis conducted by Day (1983) (Table 4-7). Unlike previous analyses which used eight elevation ranges, the distribution pattern was only analysed in seven elevation ranges because only one sinkhole was located at > 210 m altitude. In this study, both indices result in the same classification (random vs. clustered) for each range, except for the 150-180 m elevation range. Table 4-7 also shows that Sawada's approach always results in a stronger indication (lower value) for clustering (except for the one case of random distribution in the 0-30 m range). Of significance is the fact that the 90 to 120 m range has the strongest indication of clustering. The 90 to 120 m is the region most karstified; perhaps clustering becomes more evident as karstification advances (see discussion on 'daughters' below). This further supports the indication that karstification is age related within the middle terrace.

**Table 4-7:** Sinkhole distribution patterns for different elevation ranges.

| | This study | | | | | | | Day (1983) | | | | |
|---|---|---|---|---|---|---|---|---|---|---|---|---|
| Studied area | Porters and Trends groundwater catchments | | | | | | | Northern Barbados | | | | |
| Elevation (m) | Ds | $\overline{L_a}$ | $\overline{L_e}$ | $\overline{L_{ec}}$ | $\overline{R}$ | $\overline{R_c}$ | Pattern | Ds | $\overline{L_a}$ | $\overline{L_e}$ | $\overline{R}$ | Pattern |
| 0-30 | 1.20 | 1.25 | 0.91 | 0.89 | 1.37 | 1.40 | Random | 3.46 | 0.14 | 0.27 | 0.51 | Clustering |
| 30-60 | 3.05 | 0.38 | 0.57 | 1.12 | 0.67 | 0.34 | Clustering | 9.42 | 0.13 | 0.16 | 0.79 | Clustering |
| 60-90 | 5.65 | 0.32 | 0.42 | 1.30 | 0.76 | 0.25 | Clustering | 10.18 | 0.17 | 0.16 | 1.05 | Random |
| 90-120 | 13.71 | 0.16 | 0.27 | 1.89 | 0.59 | 0.08 | Clustering | 13.66 | 0.15 | 0.14 | 1.12 | Random |
| 120-150 | 4.02 | 0.38 | 0.50 | 1.19 | 0.76 | 0.32 | Clustering | 13.86 | 0.10 | 0.13 | 0.77 | Clustering |
| 150-180 | 2.33 | 0.85 | 0.66 | 1.14 | 1.29 | 0.75 | Random/ Clustering | 11.05 | 0.11 | 0.15 | 0.70 | Clustering |
| 180-210 | 1.87 | 0.69 | 0.73 | 1.07 | 0.95 | 0.64 | Clustering | 8.16 | 0.14 | 0.18 | 0.81 | Clustering |

Overall, $\overline{R}$ values from Day's (1983) investigation tend to be similar or larger than the $\overline{R}$ values of this study. According to the high, near unity, values of $\overline{R}$ he obtained, Day (1983) concluded that Barbados sinkholes presented a weak tendency toward clustering. In contrast to Day's view, the result of the current study (using Sawada's (2002) approach) shows a stronger tendency toward clustering. Day stated that small sinkholes with lateral dimensions of less than about 5 m were difficult to identify from aerial photography, especially in areas where the sugar cane crop was advanced in growth (the author of current study had access to a larger scale data base; small sinkholes were more easily identified). Miscounting small sinkholes can have a large influence on defining clustering because small sinkholes often develop nearby as an outcome of a well developed sinkhole. According to the sinkhole propagation model proposed by Drake and Ford (1972), the primary or first-generation sinkholes developing on major fractures have secondary or 'daughter' sinkholes clustered around them. These daughters, being clustered around the parent sinkhole, enhance overall sinkhole clustering.

#### 4. 3. 3 Distance to nearby gully segment

The spatial distribution of sinkholes and gullies (Figure 4-12) and the frequency distribution of distance ($L_{sg}$) between an individual sinkhole and the nearby gully (Figure 4-13) show the mean sinkhole-gully distance to be 161.44 m with a range of 29.51-380.96 m. The mean sinkhole-gully distance within different elevation ranges (Table 4-8) shows the mean distance decreased as elevation increased up to 120 m. A comparison with sinkhole densities within the same elevation ranges (Table 4-7) suggest that the distance between individual sinkholes and nearby gully segments increased when sinkhole density decreased. This is in contrast to the results of Day (1983) who showed a positive correlation between sinkhole density and the distance between an individual sinkhole and the nearby gully in northern Barbados. Day suggested that there is a competition between gullies and sinkholes development; runoff goes to one or the other.

On the contrary, in this study, the sinkholes investigated often develop close to gullies (Figure 4-13) and the sinkhole density increases with a decrease in the mean distance between an individual sinkhole and the nearby gully (Tables 4-7, 4-8) at elevations up to 120 m. Therefore, the competition between sinkhole or gully development is poor; this coincides with similar results obtained by Fermor (1972). Day's (1983) finding may have been the result of gully desiccation at higher altitudes and miscounting small sinkholes (Day had access to smaller scale information than the current study).

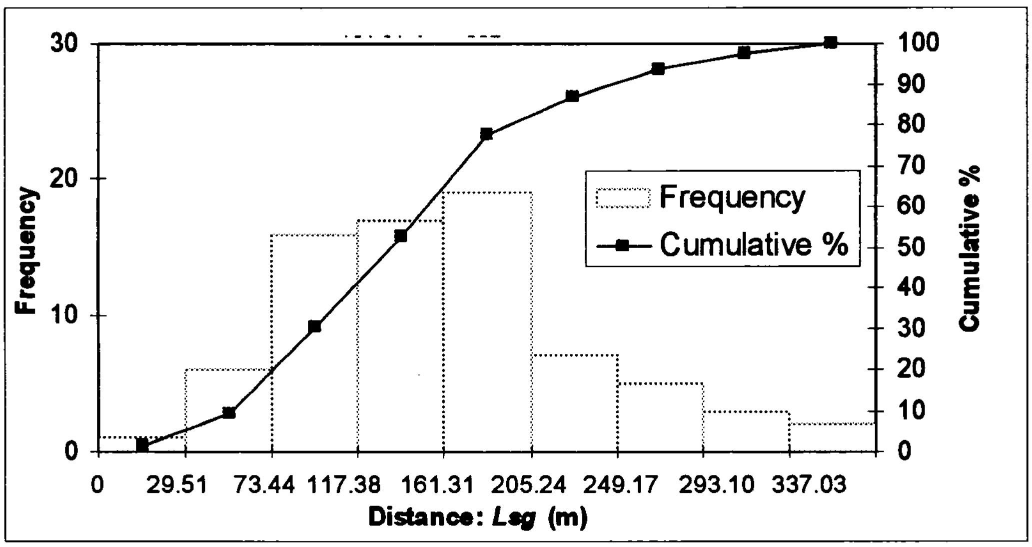


**Figure 4-13:** Frequency distribution of distance between an individual sinkhole and the nearby gully.

**Table 4-8:** Mean sinkhole-gully distance within different elevation ranges.

| Elevation (m) | 0-30 | 30-60 | 60-90 | 90-120 | 120-150 | 150-180 | 180-210 |
|---|---|---|---|---|---|---|---|
| Average distance (m) | 248.47 | 241.45 | 170.44 | 148.43 | 180.09 | 99.40 | 106.44 |
| Sinkhole density ($km^{-2}$) | 1.20 | 3.05 | 5.65 | 13.70 | 4.02 | 2.33 | 1.87 |

### 4. 3. 4 Sinkhole alignment and karst lineament

Sinkhole alignment can be defined as the orientation of a line drawn between sinkhole nearest neighbours. Karst lineament refers to the general pattern or trend of the sinkhole alignment over an area. In addition to sinkhole long-axis orientation and cluster elongation orientation as discussed above, a Rose diagram was also developed to show the alignment of neighbouring sinkholes (Figure 4-14). As in the case of sinkhole long-axis and cluster elongation orientation, there was no statistically-significant (Chi-square) orientation found in the alignment of neighbouring sinkholes, but again a northeast trend is visually discernable. The common alignment orientations fell within ranges of 60°-70 ° (16.37 % of total long-axis length) and 80°- 90° (13.52 % of total long-axis length).

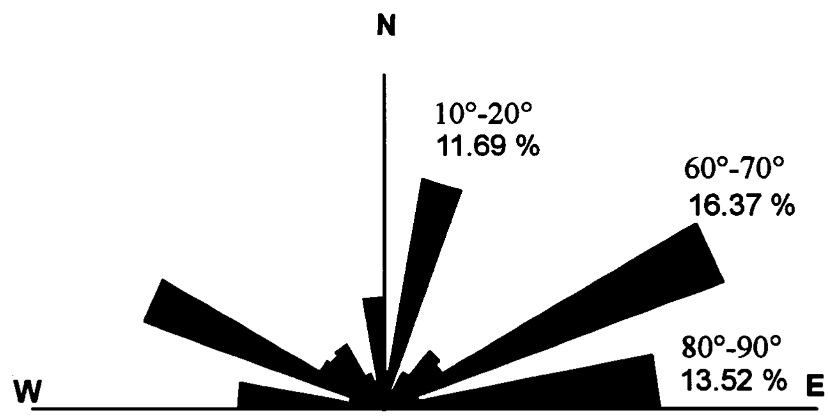


**Figure 4-14:** Rose diagram showing alignment of line drawn between nearest-neighbour sinkholes.

Modelling and mathematical approaches aside, some authors also support visual interpretation of sinkhole distribution (Chen *et al.*, 1995; Currin and Barfus, 1989; Guitérrez-Santolalla *et al.*, 2005; Hung *et al.*, 2002). With this in mind, as shown in Figure 4-15, the sinkholes in the karst area under study are visually aligned as strings of depressions (lines drawn so as not to cross gullies). The resulting karst lineament tends to be parallel to gullies / perpendicular to contour elevation lines resulting in a general northeast orientation. One hypothesis that can explain this somewhat consistent orientation is that structural patterns, such as the densities and orientations of fractures, joints, and conduit systems inherent in karst, influence sinkhole distribution. Examples of sinkhole-alignments / karst-lineaments consistent with fractures or faults and joints were found in western Kentucky (Kastning and Kastning, 1981) and in the New River basin of Virginia (Kastning, 1988). In the case of this study, no mapped faults or joints of the studied area are available to determine whether these lineaments tend to be orientated along such fractures.

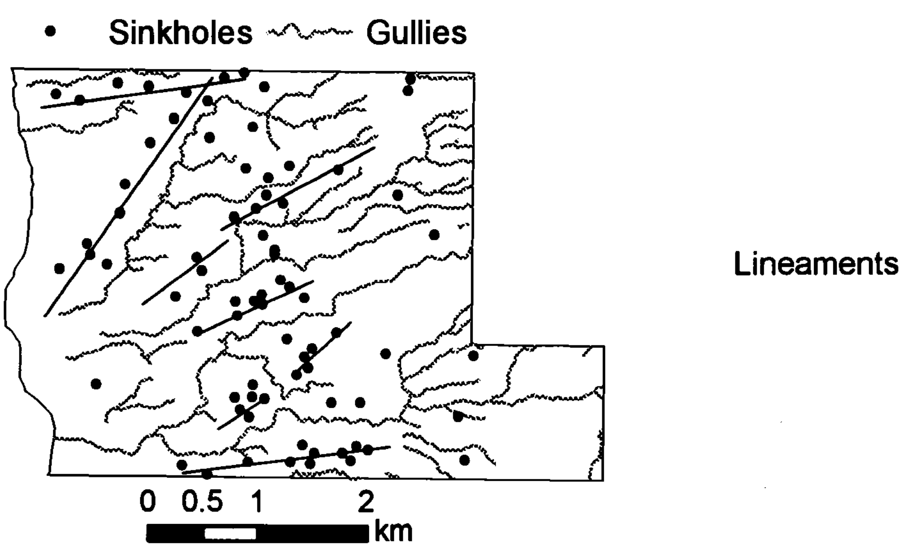


**Figure 4-15:** Sinkhole alignments / karst lineaments in the area under study.

### 4. 3. 5 The thickness of coral rock

The thickness of coral rock was examined to assess whether thickness influences sinkhole distribution. The frequency distribution of coral rock thickness at each sinkhole (Figure 4-3 and Figure 4-16) shows the mean depth to be 55.82 m (STD. = 17.46 m) and that roughly 60% of the sinkholes form where the thickness of coral rock is between 25 ~

68 m. There is no strong tendency showing that the sinkhole development in this study is constrained to a certain bedding thickness or any trend of increasing sinkhole pitting with decreasing coral rock thickness. Yet, Kastning (1989) proposed that smaller thicknesses of bedding rock (e.g., limestone) often promote large conduits, owing to the greater frequency of horizontal fractures and to mechanical breakdown of the roofs of conduits resulting in more sinkholes. Similarly the study of Gao and Alexander (2001), showed a tendency of zonation in the karst area of southeastern Minnesota where sinkholes were found only in those areas with less than 16.76 m (55 ft) in thickness. The fact that this study does not support the idea of more sinkholes in shallower coral rock emphasises the importance of multiple factors influencing sinkhole occurrence. In this study, rock infiltration seems to override rock thickness in controlling sinkhole occurrence.

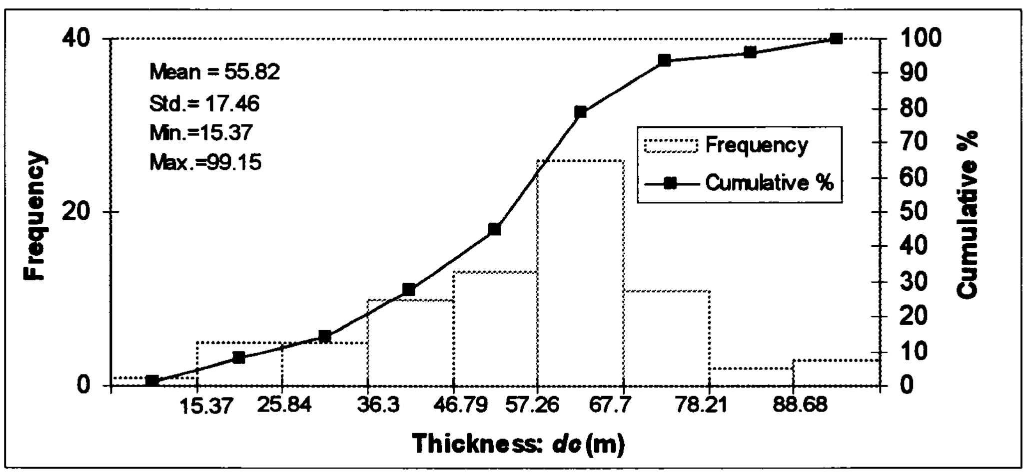


**Figure 4-16:** Frequency distribution of coral rock thickness at each sinkhole.

# CHAPTER 5 CONCLUSIONS AND SUMMARY

1. *Age and Degree of Karsitfication*: Age of karstification is not related to age a terrace. The middle terrace was the one found to be most karstified. Yet, degree of karstification within a terrace is age related. Karstification is more developed on the older ranges of the middle terrace.
2. *Shape of Sinkhole*: The planimetric shape of sinkholes tends to be symmetric and ellipsoidal. These ellipsoids become more elongated with size (age) of sinkhole. The sinkholes tend to have a northeast orientation. (For relevant results, see Figure 4-5 and Figure 4-6.)
3. *Neighbours*: Distance of neighbouring sinkholes decreases with age of coral within the middle terrace. Distance between sinkhole and nearest gully also decreases with age of coral within the middle terrace (insufficient data exist to extrapolate for the upper and lower terraces). (For relevant results, see Table 4-7 and Table 4-8.)
4. *Clusters*: Sinkholes are strongly clustered. Cluster density increases with age of coral within the middle terrace. Density of sinkholes within a cluster also increases with age of coral within the middle terrace. Statistically, the distribution of clusters is not found to be related to coral rock thickness. (For relevant results, see Table 4-7 and Figure 4-16.)
5. *Sinkholes and Gullies*: Sinkhole density increases with closeness to gullies. This suggests that 'competition' between sinkholes and gullies does not exist. This is contrary to Day's (1983) results but supportive of Fermor's (1972). (For relevant results, see Table 4-8.)

6. *Visual Interpretation; Orientation*: This study shows that sinkhole long axis, cluster elongation direction, sinkhole alignment and karst lineament all have a tendency to a northeast alignment. This supports the idea that underlying coral rock fracture and conduits have a northeast orientation. (For relevant results, see Figure 4-8, Figure 4-14, and Figure 4-15.)

## SUMMARY

This study represents an application of GIS to examine the development and distribution of karst features in the Porters and Trents groundwater catchments on the island of Barbados. The robust GIS methodology used in the study provided not only a rapid analysis of diverse spatial data, but also an objective approach for consistent measurement and calculations involved in quantifying karst landforms. Moreover, the resulting maps make it possible to visualize regional trends.

While comparing studies conducted by different authors based on various data sources (e.g., topographic maps or aerial photographic) and methods, it is found that the density of information (e.g., scale of maps, contour-interval, or resolution of photography) has an impact on the accuracy of the results. Especially when mapping small and/or shallow sinkholes. Although, a field survey can provide better determination of sinkhole dimensions, it is time consuming, restricted to the extent of area investigated and difficult in areas of dense vegetation. These challenges can be overcome by applying advanced Remote Sensing technologies and photogrammetric skills to acquire geomorphometric data across large areas while using less time.

It is recommended that future work apply similar methodologies to other regions of Barbados to ascertain effects of the development of karst surface features on groundwater flow. It is also recommended to restrict urban development, especially industrial, in the 90-120 m elevation range because of its high intensity of sinkhole clustering, sinkhole density and infiltration rate. Pollutants can be transmitted rapidly to underlying aquifers. Of course, combining such remote sensing analysis with geochemical tests (e.g., dye tracing) and geophysical exploration (e.g., electromagnetic surveys) will be even more beneficial for delineation of hazardous zones so as to ensure sustained potable water resources. Additional spatial data regarding hydro-geologic information such as cave passages and spring locations is also essential to integrate into an inclusive karst database for future groundwater development and management.

## REFERENCES


Abdullah, W. A., & Mollah, M. A. (1997). Sinkhole investigation: An on-going case study in Kuwait: *The Proceedings of the 6th Multidisciplinary conference on Sinkholes and the Engineering and Environmental Impacts of Karst.* Springfield, Missouri: PELA.

ASTM. (2002). Standard guide for conceptualization and characterization of groundwater systems. *Annual Book of A.S.T.M. Standards* (Vol. 04.09).

Bahtuarevic, A. (1989). Sinkhole density of the forest city quadrangle: *Proceeding of 3rd Multidisciplinary conference on Sinkholes.* St. Petersburg Beach, Florida: PELA

Barbados 1:2500 (Cartography). (1977). Ministry of Overseas Department, British Governemnt.

Barlow, C. A., & Ogden, A. E. (1982). A statistical comparison of joint, straight cave segment, and photo-lineament orientations. *NSS Bulletin,* 44, 107-110.

Bates, R. L., & Jackson, J. (1987). *Glossary of Geology.* Alexandria, Virginia: American Geological Institute.

Bernitz, F. S. (2000). Barbados: Helping to sustain a water supply for future generations. Retrieved June 20, 2004, from the World Wide Web: www.ionics.com/pdf/AP6258EUS.pdf

Brodie, R. S. (1998). Integrating GIS and RDBMS technologies during construction of regional groundwater model. *Environmental Modelling & Software,* 14, 119-128.

Brook, G.A., Allison T. L. (1986). Fracture mapping and ground subsidence susceptibility modeling in covered karst terrain: The example of Dougherty Country, Georgia. *Land Subsidence,* 151, 595-605.

Chen, J., Thomas, G., & Upchurch, S. (1995). Groundwater quality reflect karst development: A case study in Central-West Florida: *Proceedings of the 5th Multidisciplinary conference on Sinkholes and the Engineering and Environmental Impacts of Karst.* Gatlinburg, Tennessee: PELA.

Chen, S. (2005). Rose Diagram (Version for ArcGIS 9.x) [Visual Basic script]: ESRI. Retrieved Dec. 12, 2005, from the World Wide Web: arcscripts.esri.com/details.asp?dbid=13473.

Chen, X. (1992). *Application of Remote Sensing and GIS Techniques for Environmental Geologic Investigation, Northeast Iowa.* Unpublished dissertation, University of Iowa, Iowa.

Chenoweth, M. S. (2003). *Developing a Spatial Database for the Interpretation on Karst Landscape and Vegetation in the Jamaican Cockpit Country.* Unpublished dissertation, University of Wisconsin, Milwaukee.

Chirico, P. G. (2004). An evaluation of SRTM, ASTER and contour based DEMs in the Caribbean region: *Proceedings of the URISA 2004 Caribbean GIS conference.* Barbados: URISA.

Clark, P.J. & F.C. Evans (1954). Distance to nearest neighbour as a measure of spatial relationships in populations. *Ecology*, 35, 445-453

Coleman, A. M., & Balchin, W. G. V. (1959). The origin and development of surface depressions in the Mendip Hills: *Proc. Geol. Ass.*, 70, 291-309.

Cooper, A. H., Farrant, A. R., Adlam, K. A. M., & Walsby, J. C. (2001). The development of a national geographic information system (GIS) for British karst geohazards and risk assessment: *Proceedings of the 8th Multidisciplinary conference on Sinkholes and the Engineering and Environmental Impacts of Karst.* Harrisburg/Hershey, Pennsylvania: PELA.

Cramer, H. (1941). Die systematik der karst dolinen. *Neves Jb. Miner. Geol. Palaont.*, 85, 293-382.

Currin, J. L. & Barfus, B. L. (1989). Sinkhole distribution and characteristics in Pasco County, Florida: *Proceedings of the 3th Multidisciplinary conference on Sinkholes and the Engineering and Environmental Impacts of Karst.* St. Petersburg Beach, Florida: PELA.

Cvijic, J. (1957). Underground hydrology and morphological evolution of karst. In *Special Edition of the Serbian Geographical Society* (reprint of 1918 edition, Grenoble, France ed., Vol. 35). Beograd.

Day, M. (1978). Morphology and distribution of residual limestone hills (Mogotes) in the karst of northern Puerto Rico. *Bull. Geol. Soc. Am.*, 89, 426-432.

Day, M. (1983). Doline morphology and development in Barbados. *Annals of the Association of American Geographers,* 73(2), 206-219.

Denizman, C. (2003). Morphometric and spatial distribution parameters of karstic depressions, Lower Suwannee River Basin, Florida. *Journal of Cave and Karst Studies,* 65(1), 29-35.

Denizman, C. & Randazzo, A.F. (2000). Post-miocene subtropical karst evolution, Lower Suwannee River basin, Florida. *GSA Bulletin,* 112, 1804-1813.

Diane, F. (2000). *Morphometric Analysis of Sinkholes in Greenbrier County, West Virginia.* Unpublished master project report, West Virginia University, Morgantown.

Dimadi, A., & M.Tsakiri-Strati. (2004). Integrated use of TM image, DTM and 3D visualization in groundwater studies on karstified Marbles: *Proceedings of the XX$^{th}$ ISPRS congress: Geo-imagery Bridging Continents*. Istanbul: ISPRS.

Doerfliger, N., Jeannin, P. Y., & Zwahlen, F. (1999). Water vulnerability assessment in karst environments: A new method of defining protection areas using a multi-attribute approach and GIS (Epik method). *Environmental Geology*, 39(2), 165-168.

Drake, J., & Ford, D. C. (1972). The analysis of growth patterns of two generation populations: The example of karst sinkholes. *Can. Geog.*, 16, 381-384.

Dreiss, S. J. (1984). Effects of lithology on solution development in carbonate aquifers. *Journal of Hydrology*, 70, 295-308.

ESRI (2005). Geographic Information System. Retrieved June 20, 2005, from the World Wide Web: www.esri.com/getting_started/index.html

Elhatip, H. (1997). The influence of karst features on environmental studies in Turkey. *Environmental Geology*, 31(1/2), 27-33.

Farrell, D. A., Sandberg, S. K., Mayers, B. L., Sutherland, A., & Barnes, H. (2002). Barbados Pilot Site Characterization: Part 1. *Regional Evaluation of Saltwater Intrusion of Coast Aquifer on Caribbean Islands*. Unpublished report. Retrieved May 12, 2005, from the World Wide Web: scitec.uwichill.edu.bb/OAS/Reports/Barbados/Barbados%20Pilot%20Site%20Characterisation%202002.pdf

Fermor, J. (1972). The dry valleys of Barbados: A critical review of their pattern and origin. *Transactions of the Institute of British Geographers*, 57, 153-165.

Florea, L. J., & Paylor, R. L. (2002). Karst GIS advances in Kentucky. *Journal of Cave and Karst Studies*, 64(1), 58-62.

Ford, D. C. (1984). Karst groundwater activity and landform genesis in modern permafrost regions of Canada. In R. G. L. Fleur (Ed.), *Groundwater as a Geomorphic Agent* (pp. 340-350). London: Allen & Unwin.

Ford, D. C., & Williams, P. W. (1989). *Karst Geomorphology and Hydrology*. London: Unwin Hyman.

Gao, Y. (2002). *Karst Feature Distribution in South-eastern Minnesota: Extending GIS-Based Database for Spatial Analysis and Resource Management.* Unpublished dissertation, University of Minnesota, Minnesota.

Gao, Y., & Alexander, E. C. (2001). Application of GIS technology to study karst features of south-eastern Minnesota. In Beck & Herring (Eds.), *Geotechnical and*

*Environmental Application of Karst Geology and Hydrology*. Lisse: Swets & Zeitlinger.

Gao, Y., Alexander, E. C., & Tipping, R. G. (2002). The development of karst feature database for south-eastern Minnesota. *Journal of Cave and Karst Studies*, 64(1), 51-57.

GEO Barbados (2000). *State of the Environment Report*. Retrieved May 20, 2005, from the World Wide Web: www.rolac.unep.mx/dewalac/eng/barbados.pdf

Green, J. A., Marken, W. J., Alexander, E. C., & Alexander, S. C. (2002). Karst unit mapping using geographic information system technology, Mower County, Minnesota, U.S.A. *Environmental Geology*, 42, 457-461.

Gutiérrez-Santolalla, F., Gutiérrez-Elorza, M., Marin, C., Desir, G., & Maldonado, C. (2005). Spatial distribution, morphometry and activity of La Puebla de Alfindén sinkhole field in the Ebro river valley (NE Spain): Applied aspects for hazard zonation. *Environmental Geology*, 48 (3), 360-369.

Gyoobum, K. (2004). Lineament analysis (Version ArcView 3.x) [Avenue]: ESRI. Retrieved May 12, 2005, from the World Wide Web: arcscripts.esri.com/details.asp?dbid=13579.

Harbaugh, A., Banta, E., & Winston, R. (2006). Modflow. Retrieved Jan 10, 2006, from the World Wide Web: water.usgs.gov/nrp/gwsoftware/modflow2005/modflow2005.html.

Hubbard, D. A. (Catographer). (1988). Selected karst features of the Central Valley and Ridge Rovince, Virgina.

Horton, R. E. (1945). Erosion development of streams and their drainage basins. *Bull. Geol. Soc. Am.*, 56, 275-307.

Hung, L. Q., Dinh, N. Q., Batelaan, O., Tam, V. T., & Lagrou, D. (2002). Remote sensing and GIS-based analysis of cave development in the Suoimuoi Catchment (Son La - NW, Vietnam). *Journal of Cave and Karst Studies*, 64(1), 23-33.

Hutchinson M.F. (1989). A new method for gridding elevation and stream line data with automatic removal of pits. *Journal of Hydrology*, 106, 211-232.

Jennings, J. N. (1975). Doline morphometry as a morphogenetic tool: New Zealand examples. *N. Z. Geography.*, 31, 6-28.

Jennings, J. N. (1985). *Karst Geomorphology*. New York: Basil Blackwell Inc.

Jones, I. C. (2003). Hydro-geologic and climatic influences on spatial and inter-annual variation of recharge to a tropical karst island aquifer. *Water Resources Research*, 39(9), 1-10.

Jones, I. C., Banner, J. L., & Humphrey, J. D. (2000). Estimating recharge in a tropical karst aquifer. *Water Resources Research*, 36(5), 1289-1299.

*Karst Inventory Standards and Vulnerability Assessment Procedures for British Columbia*. (2001). Victoria, B.C.: B.C. Min. Forest.

*Karst Management Handbook for British Columbia*. (2003). Victoria, B.C.: B.C. Min. Forests.

Kastning, E. H. (1975). Cavern development in the Helderberg Plateau, east-central New York. *New York Cave Survey Bulletin*, 1, 194 p.

Kastning, E. H. (1983). *Geomorphology and Hydrogeology of the Edwards Plateau Karst, Central Texas*. Unpublished dissertation, The University of Texas, Austin.

Kastning, E. H. (1988). Karst of the New River drainage basin. In Kardos, A. R. (Ed.), *Proceedings of the Seventh New River Symposium*, Oak Hill, West Virginia (pp. 39-49). New River George National River, Oak Hill, West Virginia.

Kastning, E. H. (1989). Surficial karst patterns: Recognition and interpretation. *Proceedings of 3rd Multidisciplinary conference on Sinkholes and the Engineering and Environmental Impacts of Karst*. St. Petersburg beach, Florida: PELA.

Kastning, K. M., & Kastning, E. H. (1981). Fracture control of dolines, caves, and surface Drainage: Mississippian Plateau, Western Kentucky, U.S.A. In B. F. Beck (Ed.), *Proceedings of the 8th International Congress of Speleology, Bowling Green, Kentucky* (Vol. 2, pp. 696-698). Huntsville, Alabama: National Speleological Society.

Kemmerly, P. R. (1976). Definitive doline characteristics in the Clarksville quadrangle, Tennessee. *Bull. Geol. Soc. Am.*, 87, 42-46.

Kemmerly, P. R. & Towe, S. K. (1978). Karst depressions in a time context. *Earth Surficial Processes*, 3, 355-362.

Kemmerly, P. R. (1980). A time-distribution study of doline Collapse: Framework for prediction. *Environmental Geology*, 3, 123-130.

Kemmerly, P. R. (1982). Spatial analysis of a karst depression population: Clues to genesis. *Geol. Soc. Am. Bull*, 93, 1078-1086.

Khawam, W. (2004). *Water Demand Management in the Caribbean: A Case Study of Barbados*. Unpublished dissertation, McGill University, Montreal.

Kiraly, L. (2003). Karstificaiton and groundwater flow. *Speleogenesis and Evolution of Karst Aquifers*, 1(3), 1-26. Retrieved June 12, 2005, from the World Wide Web: www.speleogenesis.info/pdf/SG3/SG3_artId3244.pdf

Klohn, C. (1998). *Report on Task 12: Development and Management Plan for the Water Resources Management and Water Loss Study*: Government of Barbados.

LaMoreaux, P. E., Powell, W. J., & LeGrand, H. E. (1997). Environmental and legal aspects of karst areas. *Environmental Geology*, 29(1/2), 23-36.

Lane, S. N., Chandler, J. H., & Richards, K. S. (1996). Landform monitoring, modelling and analysis: Landform in geo-morphological Research. In S. N. Lane, K. S. Richards & J. H. Chandler (Ed.), *Landform Monitoring, Modelling and Analysis* (pp. 1-17). John Wiley & Sons Ltd.

LaValle, P. (1967). Some aspects of linear karst depression development in south-central Kentucky. *Assoc. Am. Geographics Annals*, 2, 49-71.

Lei, M., Jiang, X., & Li, Y. (2001). New advances of karst collapse research in China: *Proceedings of the 8th Multidisciplinary conference on Sinkholes and the Engineering and Environmental Impacts of Karst*. Harrisburg/Hershey, Pennsylvania: PELA.

Lindsay, J. B. (2004). The terrain analysis system: A tool for hydro-geomorphic applications. *Hydrological Processes*, 19(5), 1123-1130.

Littlefield, J. R., Culbreth, M. A., Upchurch, S. B., & Stewart, M. T. (1984). Relationship of modern sinkhole development to large scale photo-linear features: *Proceedings of the 1st Interdisciplinary conference on Sinkholes*. Orlando, FL: Florida Sinkhole Research Institute.

Marchetti, M., & Rivas, V. (2001). *Geomorphology and Environmental Impact Assessment*. A.A. Balkema.

Mesolella, K. J. (1967). Zonation of uplifted pleistocene coral reefs in Barbados. *Science*, 156, 638-640.

Milanovic, P. T. (2004). *Water Resources Engineering in Karst*. Boca Raton, Florida: CRC Press LLC.

Miller, R. A. (Cartographer). (1977). Geologic hazards maps of Tennessee [Sheet 1].

Mills, H. H., & Starnes, D. D. (1983). Sinkhole morphometry in a fluviokarst region: Eastern Highland Rim, Tennessee, U.S.A. *Z. Geomorph. N. F.*, 17, 39-54.

Moore, H. L. (1976). Drainage problems in carbonate terrane of East Tennessee. *Proceedings of the TN Dept. of Transportation conference*. Nashville, TN.

Moore, H. L. (1981). Karst problems along Tennessee highways: An overview. *Proceedings of the 31st Highway Geology Symposium*. Austin, TX: Texas Bureau of Economic Geology.

Moore, H. L. (1987). Sinkhole development along untreated highway ditchlines in East Tennessee. *Proceedings of the 2nd Multidiscipline conference on Sinkholes and the Environmental Impacts of Karst*. Orlando, FL: Florida Sinkhole Res. Institute.

Moore, R., Oderson, D., & Singh, A. D. (2003). *Barbados National Assessment Report*: Government of Barbados.

Nelson, J. W. (1988). Influence of joints and fractures upon the hydrogeology of karst terrane: *Proceedings of the International conf. on Fluid Flow in Fractured Rocks.* Franklin, Co., Albabama: U.S.G.S.

Ogden, A. E., Curry, W. A., & Cummings, J. L. (1989). Morphometric analysis of sinkholes and caves in Tennessee comparing the Eastern Highland Rim and Valley and Ridge physiographic provinces: *Proceedings of the 3rd Multidisciplinary conference on Sinkholes and the Engineering and Environmental Impacts of Karst.* St. Petersburg beach, Florida: PELA.

Ogden, A. E., & Reger, J. P. (1977). Use of morphometric analysis of dolines and cavern distribution for predicting ground subsidence, Monroe County, West Virginia: *Proceedings of the International Symposium on Hydrologic Problems in Karst Regions.* Bowling Green: Western Kentucky University.

Palmer, A. N. (1962). *Geology of Knox Cave System, Albany County, New York.* Unpublished dissertation, Williams College, Williamstown, Massachusetts.

Patton, T. H., & Klein, J.-G. (1989). Sinkhole formation and its effect on Peace River hydrology: *Proceedings of the 3rd Multidisciplinary conference on Sinkholes and the Engineering and Environmental Impacts of Karst.* St. Petersburg Beach, Florida: PELA.

Phelan, T. L. (2002). Public datasets integrated with GIS and 3D visualization help expand subsurface conceptual model. *Journal of Cave and Karst Studies,* 64(1), 77-81.

Quinlan, J. F. (1970). Central Kentucky karst: *Proceedings of the Actes de la Réunion Internationale Karstologie.* Languedoc-Provence: Études et traveaux de Méditeranée.

Rauch, H. W., & White, W. B. (1970). Lithologic controls on the development of solution porosity in carbonate aquifers. *Water Resources Research,* 6, 1175-1192.

Ringskog, K. (2004). International seminar: Financing water and sanitation services in the Caribbean. Retrieved May 24, 2005, from the World Wide Web: www.iadb.org/sds/conferences/waterconference/Institutions&Water-Barbados.pdf

Ryan, K. W. (1989). Two-dimensional numerical simulation of the relationship between sinkhole lakes and groundwater along the Central Florida ridge: *Proceedings of the 3rd Multidisciplinary conference on Sinkholes and the Engineering and Environmental Impacts of Karst.* St. Petersburg Beach, Florida: PELA.

Sawada, M. (2002). Nearest Neighbor Analysis [Visual basic application]: Environmental Systems Research Institute. Retrieved Sep 10, 2005, from the World Wide Web: arcscripts.esri.com/details.asp?dbid=12227.

Senn, A. (1946). *Report of the British Union Oil Co. Ltd. on the Geological Investigation of Groundwater Resources of Barbados*: B.W.I.

Shofner, G. A., Mills, H. H., & Duke, J. E. (2001). A simple map index of karstification and its relationship to sinkhole and cave distribution in Tennessee. *Journal of Cave and Karst Studies*, 63(2), 67-75.

Singh, Y. (1989). Sinkholes (dolines) in Bhander limestones around Rewa, Central India, and their environmental significance: *Proceedings of the 3th Multidisciplinary conference on Sinkholes and the Engineering and Environmental Impacts of Karst.* St. Petersburg Beach, Florida: PELA.

Soto, A. E., & Morales, W. (1984). Collapse sinkholes in the Blanket Sands of the Puerto Rico karst belt: *Proceedings of the 1st Interdisciplinary conf. on Sinkholes.* Orlando, FL: Florida sinkhole Research Institute.

Strahler, A. N. (1957). Quantitative analysis of watershed geomorphology. *Trans. Am. Geophys. Union*, 38, 913-920.

Szukalski, B. W. (2002). Introduction to cave and karst GIS. *Journal of Cave and Karst Studies, 64*(1), 3.

Veni, G. (2002). Revising the karst map of the United States. *Journal of Cave and Karst Studies*, 64(1), 45-50.

Voss, C. I. (2003). Saturated-unsaturated, variable-density groundwater flow with solute or energy transport (Version 2D3D1): USGS. Retrieved Jan 10, 2006, from the World Wide Web: water.usgs.gov/nrp/gwsoftware/sutra/sutra.html.

Waltham, A. C. (1989). Karst, caves and engineering: The British experience: *Proceedings of the 3rd Multidisciplinary conference on Sinkholes and the Engineering and Environmental Impacts of Karst.* St. Petersburg beach, Florida: PELA.

Wandelt, B. (2000). *Geomorphologische Detailkartierung und Chronostratigraphische Gliederung der Quartaren Korallenriffe auf Barbados (West Indies) unter Besonderer Berucksichtigung des Karstformenschatzes.* Unpublished dissertation, University of Cologne, Berlin.

Water resources and hydrogeology. (1978). *Barbados water resources study*: Stanley Associates Engineering Ltd.

White, E. L., & White, W. B. (1979). Quantitative morphology of landforms in carbonate rock basins in the Appalachian highlands. *Geological Society of American Bulletin*, 90, 385-396.

White, W. B. (1988). *Geomorphology and Hydrology of Karst Terrains*. New York: Oxford University Press, Inc.

White, W. B., Jefferson, G. L., & Haman, J. F. (1966). Quartzite karst in south-eastern Venezuela. *Internatl. J. Speleol.*, 2, 309-314.

Whitman, D., & Gubbels, T. (1999). Applications of GIS technology to the triggering phenomena of sinkholes in Central Florida: *Proceedings of the 7th Multidisciplinary conference on Sinkholes and the Engineering and Environmental Impacts of Karst*. Harrisbury-Hershey, Penn.: PELA.

Williams, P. W. (1969). The geomorphic effects of groundwater. In R. J. Chorley (Ed.), *Water, Earth and Man*. London: Methuen.

Williams, P. W. (1972a). The analysis of spatial characteristics of karst terrains. In R. J. Chorley (Ed.), *Spatial Analysis in Geomorphology* (pp. 135-163). London: Methuen.

Williams, P. W. (1972b). Morphometric analysis of polygonal karst with examples from New Guinea. *Geological Society of America bulletin*, 83, 761-796.

Wise, S. M. (1998). The effect of GIS interpolation errors on the use of digital elevation models in geomorphology. In S. N. Lane, K. S. Richards & J. H. Chandler (Eds.), *Landform Monitoring, Modelling and Analysis* (pp. 1-17). John Wiley & Sons Ltd.

# APPENDIX A

The definition of the groundwater protection zones (Khawam, 2004)

| Zone | Boundary | Max. depth of soak-away pits | Domestic control restrictions | Industrial restrictions |
|---|---|---|---|---|
| 1 | 300 days travel time | None Allowed | No new houses or water connections.<br>No changes to existing wastewater disposal | No new industrial development & quarrying. |
| 2 | 600 days travel time | 6.5 m | Septic tank of approved design. Separate soakaway pits for toilet effluent and other domestic wastewater. No storm runoff to sewage soakaway pit. No new oil tanks. | All liquid wastes to be dealt with as specified by the BWA. |
| 3 | 5-6 years travel time | 13 m | As above for domestic wastewater.<br>Petrol fuel or oil tanks with approved leak-proof design | Maximum soak-away depth as for domestic wastes |
| 4 | All highlands | No limit | No restriction on domestic wastewater disposal. Petrol fuel or oil tanks with approved leak-proof design. | No limit |
| 5 | Coastline | No limit | No restrictions on domestic wastewater disposal. Siting of new fuel storage tanks subject to approval of the Barbados Water Authority | No limit |

# APPENDIX B

Water quality of public supplies in Barbados, compared to international standards ("*GEO Barbados*", 2000)

| Parameter | International standards | Barbados mean | Catchments mean | | |
|---|---|---|---|---|---|
| | | | St. Michael | St. Philip | West Coast |
| Nitrate_N (mg $L^{-1}$) | 10 | 7.11 | 6.87 | 8.15 | 6.54 |
| Chloride (mg $L^{-1}$) | 250 | 112.6 | 63.5 | 68.7 | 183.9 |
| Sodium (mg $L^{-1}$) | 200 | 50.26 | 24.6 | 52.9 | 75.8 |
| Sulphate (mg $L^{-1}$) | 250-400 | 33.5 | 24.1 | 36.4 | 37.8 |
| pH | 8.5 | 7.6 | 7.37 | 7.35 | 7.33 |
| Atrazine (ug $L^{-1}$) | 3.0 | 0.46 | 0.38 | 0.61 | 0.37 |
| Fæcal Coliform (colonies/100ml) | < 1/100 | < 1/100 | < 1/100 | < 1/100 | < 1/100 |
| TDS* (mg $L^{-1}$) | 500 | 426 | 335 | 423 | 618 |

*TDS, total dissolved solids.

# APPENDIX C

Data bases for conceptualization and characterization of groundwater systems

| | |
|---|---|
| Geomorphology | Topographic maps or digital elevation model, or both<br>Drainage trace map |
| Geology | Geologic map and stratigraphic column<br>Surficial geology map and stratigraphic column<br>Geologic cross sections<br>Lithologic or driller's logs, or both |
| Geophysics | Gravity maps and data<br>Magnetic maps and data<br>Resistivity maps and data<br>Seismic and earthquake activity maps and data<br>Electromagnetic induction data |
| Meteorology and Climate | Precipitation data<br>Temperature data<br>Evaporation data<br>Solar radiation data |
| Vegetation | Vegetation type and distribution maps<br>Consumptive water use data |
| Soils | Soil type and characteristics maps<br>Soil properties data |
| Hydrology | Water well data<br>Potentiometric surface maps<br>Springs and seeps data<br>Surface water data<br>Aquifer properties data |
| Hydrochemistry /Geochemistry | Isotope hydrochemistry<br>Organic hydrochemistry<br>Inorganic hydrochemistry<br>Soil, chemical precipitates, and rock geochemistry |
| Anthropogenic aspects | Political boundaries maps<br>Land ownership maps<br>Land use-Land cover maps including historical information, if available |
| Hydro-geologic characterization | Hydro-geologic table of attributes<br>Hydro-geologic maps<br>Hydro-geologic cross-section and stratigraphic columns |
| Groundwater characterization | Groundwater system tables for recharge/discharge types and amount<br>Groundwater system maps showing recharge/discharge, and flow system<br>Groundwater system cross sections showing recharge/discharge, and flow system<br>Potentio-metric surface maps for each hydrologic layer |

# APPENDIX D

Lithologic records were extracted by the BWA from monitored borehole/drill wells (elevation is referenced to sea level).

| Well no. | Borehole no. | Name of the location | Geographic coordinate (BNG, m) X | Y | Z | Type of lithology | Elevation (m) |
|---|---|---|---|---|---|---|---|
| 1 | 53 | Norwood | 23322.89 | 74064.60 | 100.34 | Medium hard coral | 94.86 |
| | | | | | | Fairly hard coral | 81.18 |
| | | | | | | Medium hard coral | 72.06 |
| | | | | | | Fairly hard coral | 47.74 |
| | | | | | | Medium hard coral | 44.70 |
| | | | | | | Very hard coral | 36.18 |
| | | | | | | Oceanics | 18.24 |
| 2 | 54 | Molyneux #1 | 23199.11 | 75215.48 | 94.26 | Fairly hard coral | 69.93 |
| | | | | | | Very hard coral | 36.79 |
| | | | | | | Oceanics | 36.49 |
| 3 | 55 | Molyneux #2 below cliff | 22734.18 | 75210.00 | 71.45 | Fairly hard coral | 62.33 |
| | | | | | | Very hard coral | 56.86 |
| | | | | | | Medium hard coral | 30.41 |
| | | | | | | Fairly hard coral | 21.89 |
| | | | | | | Medium hard coral | -0.91 |
| | | | | | | Fairly hard coral | -1.82 |
| | | | | | | Oceanics | -2.13 |
| 4 | 56 | Lacelles | 23219.35 | 75755.14 | 100.34 | Medium hard coral | 64.46 |
| | | | | | | Oceanics | 38.31 |
| 5 | 57 | Blowers Plantation | 23329.07 | 76243.94 | 110.98 | Very hard coral | 101.86 |
| | | | | | | Sandy | 94.26 |
| | | | | | | Fairly hard coral | 85.74 |
| | | | | | | Medium | 80.57 |
| | | | | | | Fairly hard coral | 62.94 |
| | | | | | | Oceanics | 48.65 |

## APPENDIX D (cont.)

| Well no. | Borehole no. | Name of the location | Geographic coordinate (BNG, m) X | Y | Z | Type of lithology | Elevation (m) |
|---|---|---|---|---|---|---|---|
| 6 | 59 | Trents #1 | 22375.68 | 76383.17 | 60.81 | medium hard coral | 50.78 |
| | | | | | | sandy with hard spots | 44.70 |
| | | | | | | fairly hard coral | 36.49 |
| | | | | | | very hard coral | 27.36 |
| | | | | | | oceanics | 7.30 |
| 7 | 58 | Blowers Plantation #2 | 22661.89 | 76000.49 | 79.05 | Medium hard coral | 73.58 |
| | | | | | | Fairly hard coral | 59.90 |
| | | | | | | Medium hard coral | 50.78 |
| | | | | | | Fairly hard coral | 26.45 |
| | | | | | | Medium hard coral | 23.41 |
| | | | | | | Oceanics | 14.59 |
| 8 | 60 | Trents #2 | 22429.75 | 76802.53 | 68.41 | Soil | 67.96 |
| | | | | | | Medium hard coral | 49.26 |
| | | | | | | Sandy | 46.22 |
| | | | | | | Very hard coral | 40.13 |
| | | | | | | Oceanics | 2.13 |
| 9 | 61 | Mount Standfast Plantation #1 | 22488.09 | 77661.73 | 72.97 | fairly hard coral | 64.46 |
| | | | | | | very hard coral | 59.29 |
| | | | | | | fairly hard coral | 39.53 |
| | | | | | | very hard coral | 37.09 |
| | | | | | | fairly hard coral | 31.62 |
| | | | | | | very hard coral | 27.97 |
| | | | | | | fairly hard coral | 19.76 |
| | | | | | | very hard coral | 16.72 |
| | | | | | | fairly hard coral | 13.68 |
| | | | | | | medium hard coral | 12.16 |
| | | | | | | fairly hard coral | 7.60 |
| | | | | | | oceanics | 6.08 |

## APPENDIX D (cont.)

| Well no. | Borehole no. | Name of the location | Geographic coordinate (BNG, m) X | Y | Z | Type of lithology | Elevation (m) |
|---|---|---|---|---|---|---|---|
| 10 | 62 | Mount Standfast #2 | 22155.20 | 77355.05 | 50.17 | very hard coral | 47.74 |
| | | | | | | fairly hard coral | 46.52 |
| | | | | | | very hard coral | 44.70 |
| | | | | | | fairly hard coral | 42.57 |
| | | | | | | medium hard coral | 35.57 |
| | | | | | | very hard coral | 32.53 |
| | | | | | | fairly hard coral | 29.49 |
| | | | | | | very hard coral | 25.84 |
| | | | | | | medium hard coral | 22.80 |
| | | | | | | fairly hard coral | 19.76 |
| | | | | | | medium hard coral | 9.73 |
| | | | | | | fairly hard coral | 2.13 |
| | | | | | | very hard coral | -2.43 |
| | | | | | | fairly hrad coral | -4.56 |
| | | | | | | very hard coral | -10.64 |
| | | | | | | fairly hard coral | -18.24 |
| | | | | | | oceanics | -18.85 |
| 11 | 63 | Mount Standfast #3 in gully east of house. | 22089.02 | 77745.59 | 43.78 | soil | 43.33 |
| | | | | | | medium hard coral | 30.10 |
| | | | | | | fairly hard coral | -9.43 |
| | | | | | | very hard coral | -13.99 |
| | | | | | | oceanics | -31.01 |
| 12 | 64 | Mount Standfast #4 north of plantation in cart road. | 21791.85 | 78028.41 | 56.55 | medium hard coral | 42.87 |
| | | | | | | fairly hard coral | 31.32 |
| | | | | | | very hard coral | 28.28 |
| | | | | | | fairly hard coral | -4.26 |
| | | | | | | oceanics | -7.30 |

# APPENDIX D (cont.)

| Well no. | Borehole no. | Name of the location | Geographic coordinate (BNG, m) X | Y | Z | Type of lithology | Elevation (m) |
|---|---|---|---|---|---|---|---|
| 13 | 65 | Mount Standfast #5 on public road north east plantation. | 22032.74 | 78126.04 | 66.28 | fairly hard coral | 60.20 |
| | | | | | | very hard coral | 54.12 |
| | | | | | | medium hard coral | 42.26 |
| | | | | | | Oceanics | 12.77 |
| 25 | | Sion Hill #1 in estate yard near dwelling house | 23592.91 | 80240.26 | 187.22 | Coral | 140.93 |
| | | | | | | Oceanics | 140.85 |
| 26 | | Sion Hill #3 on north side of gully south Sion Hill yard | 23540.20 | 79960.85 | 170.27 | Coral | 128.69 |
| 28 | 76 | Carlton #1 330m east of Carlton House | 22084.96 | 79895.06 | 72.36 | fairly hard coral rock | 58.38 |
| | | | | | | medium hard coral rock | 42.57 |
| | | | | | | farily hard coral rock | 39.22 |
| | | | | | | Oceanics | 26.45 |
| 29 | 77 | Carlton #2 | 22087.39 | 80144.97 | 56.25 | fairly hard coral rock | 42.57 |
| | | | | | | medium hard coral rock | 24.32 |
| | | | | | | fairly hard coral rock | 8.51 |
| | | | | | | oceanics | 8.51 |
| 30 | | Greenwich (former Hope, Mr. Cecil Jemmott) in estate yard | 22861.15 | 76958.29 | 102.16 | coral | 35.88 |
| 31 | 79 | Carlton #4 | | | 54.34 | soil | 53.43 |
| | | | | | | very hard coral rock | 49.78 |
| | | | | | | fairly hard coral rock | 26.98 |
| | | | | | | medium hard coral rock | -2.21 |
| | | | | | | fairly hard coral rock | -18.63 |
| | | | | | | oceanics | -18.63 |

## APPENDIX D (cont.)

| Well no. | Borehole no. | Name of the location | Geographic coordinate (BNG, m) X | Y | Z | Type of lithology | Elevation (m) |
|---|---|---|---|---|---|---|---|
| 32 | 83 | Norwood #2 (at north entrance to plantation house) | 22868.21 | 74598.87 | 85.74 | medium hard coral rock with few soft spots | 62.03 |
| | | | | | | fairly hard coral rock | 58.38 |
| | | | | | | medium hard coral rock | 44.70 |
| | | | | | | very hard coral rock | 35.57 |
| | | | | | | medium hard coral rock | 24.02 |
| | | | | | | fairly hard coral rock | 14.29 |
| | | | | | | oceanics | 8.21 |
| 33 | 82 | Molyneux (in plantation yeard next to the old mill tower) | 22851.32 | 74918.94 | 82.09 | medium hard coral rock | 68.41 |
| | | | | | | fairly hard coral | 36.49 |
| | | | | | | very hard coral rock | 31.01 |
| | | | | | | fairly hard coral | 19.76 |
| | | | | | | very hard coral rock | 15.81 |
| | | | | | | oceanics | 13.07 |
| 34 | 81 | Seaview Road | 22538.43 | 75641.79 | 66.28 | medium hard coral rock | 35.57 |
| | | | | | | fairly hard coral rock with few soft spots | 10.03 |
| | | | | | | oceanics | 1.22 |
| 35 | 78 | Carlton #3 | 21711.94 | 80088.64 | 52.60 | medium hard coral with a few soft spots | 20.68 |
| | | | | | | fairly hard coral with a few soft spots | -8.21 |
| | | | | | | medium hard coral | -15.81 |
| | | | | | | oceanics | -30.41 |

## APPENDIX D (cont.)

| Well no. | Borehole no. | Name of the location | Geographic coordinate (BNG, m) X | Y | Z | Type of lithology | Elevation (m) |
|---|---|---|---|---|---|---|---|
| 36 | 80 | Mount Standfast #6 | 22512.22 | 78086.38 | 69.93 | medium hard coral with a few soft spots | 21.28 |
| | | | | | | oceanics | 11.25 |
| 37 | 88 | Norwood #3 | 22723.60 | 75150.12 | 82.09 | medium hard coral rock | 77.53 |
| | | | | | | sandy | 74.49 |
| | | | | | | medium hard coral rock | 62.33 |
| | | | | | | very hard coral rock with few soft spots | 44.09 |
| | | | | | | medium hard coral rock | 22.50 |
| | | | | | | fairly hard coral rock with a few soft spots | 2.13 |
| | | | | | | oceanics | -9.73 |